Enzyme-Triggered PEGylated pDNA-Nanoparticles for Controlled Release of pDNA in Tumours.

ARTICLE *in* BIOCONJUGATE CHEMISTRY · JANUARY 2013

Impact Factor: 4.51 · DOI: 10.1021/bc300419g · Source: PubMed

7 AUTHORS, INCLUDING:

Mathieu Mevel
University of Nantes
28 PUBLICATIONS **372** CITATIONS
SEE PROFILE

Carla Prata
Axolabs GmbH
26 PUBLICATIONS **598** CITATIONS
SEE PROFILE

Maya Thanou
King's College London
59 PUBLICATIONS **3,693** CITATIONS
SEE PROFILE

Andrew D Miller
King's College London
115 PUBLICATIONS **2,303** CITATIONS
SEE PROFILE

Bioconjugate Chemistry

Article

pubs.acs.org/bc

Enzyme-Triggered PEGylated pDNA-Nanoparticles for Controlled Release of pDNA in Tumors

Peerada Yingyuad,[†] Mathieu Mével,[†] Carla Prata,[†] Stefan Furegati,[†] Christos Kontogiorgis,[†] Maya Thanou,[‡] and Andrew D. Miller*[,†,‡]

[†]Imperial College Genetic Therapies Centre, Department of Chemistry, Imperial College London, London, SW7 2AZ, United Kingdom

[‡]Institute of Pharmaceutical Science, King's College London, Franklin-Wilkins Building, Waterloo Campus, 150 Stamford Street, London, SE1 9NH, United Kingdom

Supporting Information

ABSTRACT: Nanoparticle mediated functional delivery of plasmid DNA (pDNA) in vivo typically requires the formulation of pDNA-nanoparticles with a surface layer of stealth/biocompatibility polymer (usually poly(ethylene glycol) [PEG]). This PEG layer ensures the colloidal stability of pDNA-nanoparticles in biological fluids and minimizes nanoparticle interactions with the reticulo-endothelical system. Unfortunately, the presence of the PEG layer appears to contribute to a reduction in efficiency of functional delivery of pDNA once target cells are reached. For this reason, we have focused recent research efforts on "triggerable" nanoparticle systems. These are designed to be stable from the point of administration until a target site of interest is reached, then triggered for the controlled release of therapeutic agent payload(s) at the target site by changes in local endogenous conditions or through the application of some exogenous stimulus. Here, we describe investigations into the potential use of enzymes to trigger pDNA-mediated therapy through a process of enzyme-assisted nanoparticle triggerability. Our approach is to use PEG^{2000}-peptidyl lipids with peptidyl moieties sensitive to tumor-localized elastase or matrix metalloproteinase-2 digestion, and from these prepare putative enzyme-triggered PEGylated pDNA-nanoparticles. Our results provide initial proof of concept in vitro. From these data, we propose that this concept should be applicable for functional delivery of therapeutic nucleic acids to tumor cells in vivo, although the mechanism for enzyme-assisted nanoparticle triggerability remains to be fully characterized.

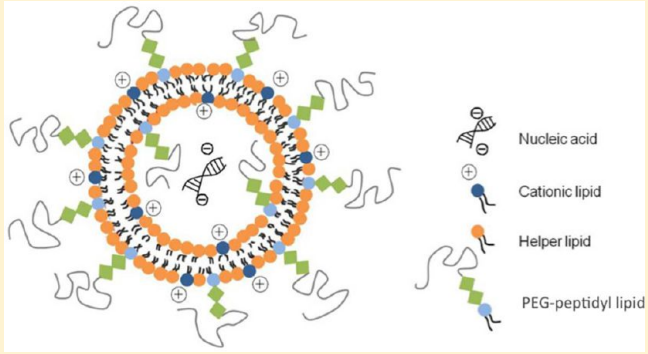

INTRODUCTION

The design of appropriate nanoparticles for the functional delivery of plasmid DNA (pDNA) to target cells in vivo has been a main objective of gene therapy research over the past few years. Starting originally with cationic liposomes, pDNA-lipoplex nanoparticles were found too unstable with respect to colloidal aggregation in vivo to be of real utility.[1] Although several means were devised to create more stable lipoplex nanoparticles,[2−5] we have been forced to come to the conclusion that our preferred approach going forward should be through the formation of lipid-based nanoparticles that conform to the synthetic, self-assembly **ABCD** nanoparticle paradigm as described previously.[6−8]

Nanoparticles of this type are equipped with a surface layer (**C**-layer)[6−8] of poly(ethylene glycol) [PEG]) that is known to provide for colloidal stability in biological fluids and resistance to immune system challenge. However, functional delivery of entrapped nucleic acids can be affected substantially at target sites by the presence of a PEG surface layer too.[6−8] This situation represents a potentially significant internal nanoparticle barrier to successful functional delivery that requires a response. In our case, we have sought to overcome this problem with a focus on the development of nanoparticles that are triggerable (i.e., stable in biological fluid, but triggered for the controlled release of therapeutic agent payload(s) at the target sites of interest by changes in local endogenous conditions or through the application of some exogenous stimulus). In this respect, we very recently described two forms of triggerable nanoparticle for the functional delivery of pDNA to murine lung in vivo. The first system was categorized as a half-life-triggered lipid-based nanoparticle system,[9] and the second as a redox-triggered polymer-based nanoparticle system.[10] Here, we describe our efforts to devise enzyme-triggered lipid-based pDNA-nanoparticles for enhanced transfection of tumor cells, taking advantage of the binding and cleavage specificity of tissue-matrix associated enzymes, such as human leukocyte elastase (HLE) and matrix metalloproteinase-

Received: July 28, 2012
Revised: December 19, 2012
Published: January 10, 2013

   dx.doi.org/10.1021/bc300419g | *Bioconjugate Chem.* 2013, 24, 343−362

Scheme 1. Human Leukocyte Elastase (HLE) and Matrix Metalloproteinase-2 (MMP-2) Mechanisms[a]

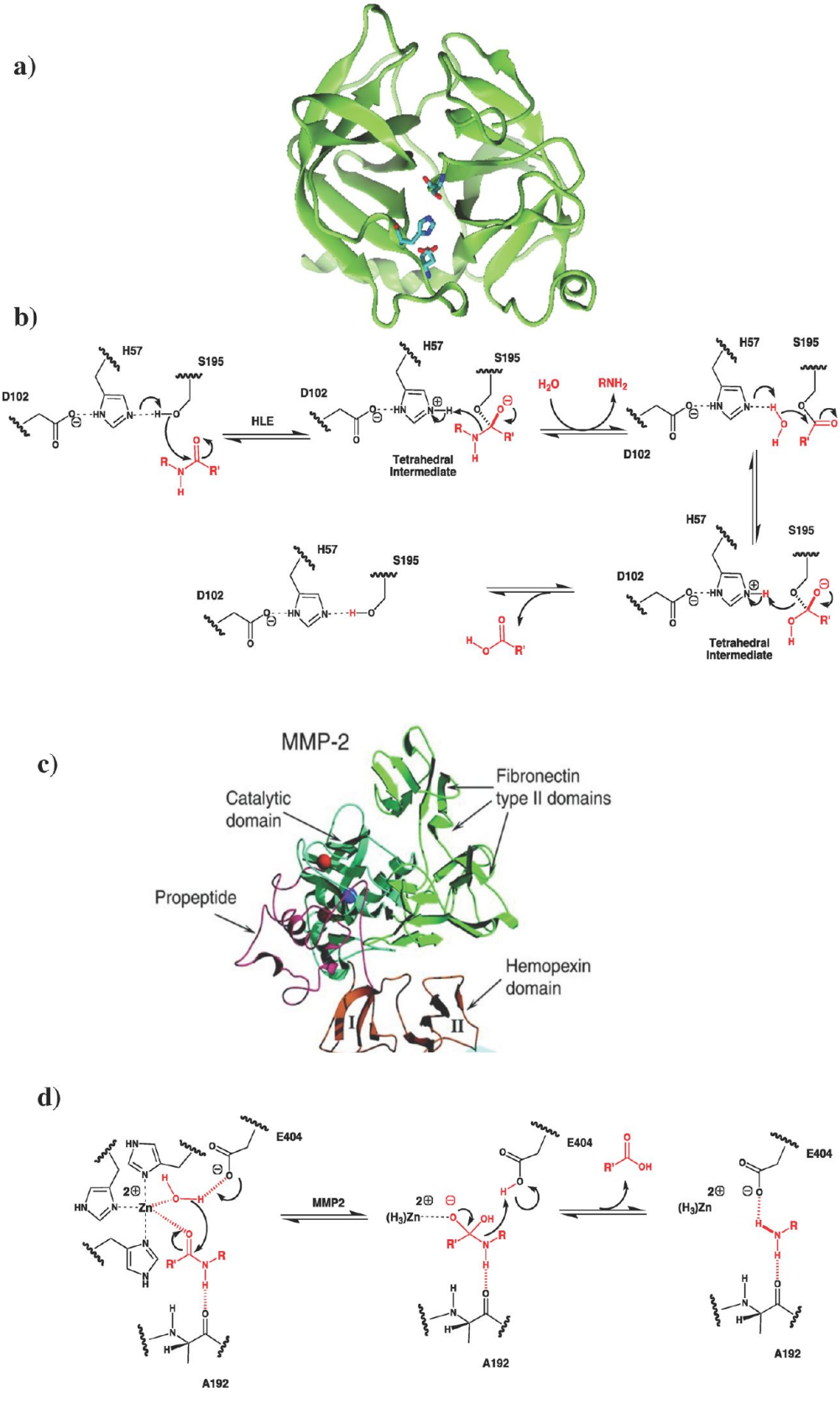

[a](a) crystal structure of human leukocyte elastase is shown (PDB: 1EAS); (b) the peptide link hydrolysis mechanism is shown involving the catalytic triad, His57, Asp102, and Ser195; (c) representation of the complex between pro-MMP-2/tissue inhibitor of metalloproteinase-2 (TIMP-2). The domain structure of MMP-2 is shown[19] (PDBs: 1HOV and 1GXD); (d) mechanism of catalytic Zn(II) mediated peptide link hydrolysis is shown involving Ala 192 and Glu404.

dx.doi.org/10.1021/bc300419g | *Bioconjugate Chem.* 2013, 24, 343−362

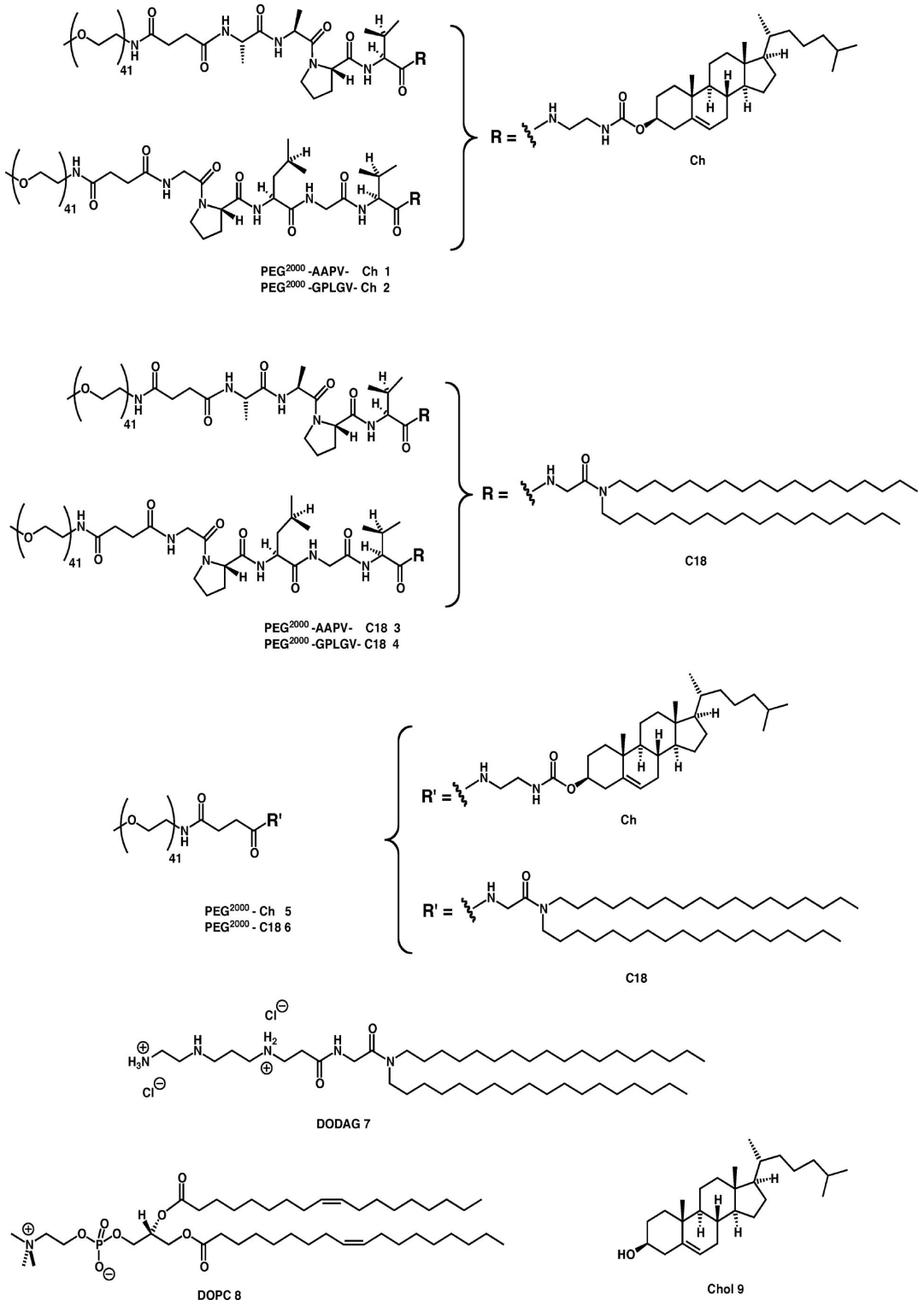

Figure 1. Lipids used in preparation of cationic liposomes.

2 (MMP-2) that are present in the extracellular spaces of tumor volumes.

High levels of the proteolytic enzyme, elastase, are found in tumors in order to promote invasion and metastasis by degrading basement membrane and extracellular matrix barrier.[11−13] On the other hand, many tumors are also well-known to secrete substantial quantities of MMP-2 for the degradation of the intercellular collagen matrix in order to promote invasion and metastasis (Scheme 1).[14−21] Upon the basis of amino acid residue proteolysis-consensus sequences for these two enzymes, we synthesized four different PEG^{2000}-peptidyl-lipids **1**−**4** and two PEG^{2000}-lipid controls **5** and **6** (Figure 1) that were then used in the formulation of PEGylated pDNA-nanoparticles. We report on data from a sequence of nanoparticle characterization experiments and also from studies involving functional nucleic acid delivery to two tumor cell lines

dx.doi.org/10.1021/bc300419g | *Bioconjugate Chem.* 2013, 24, 343−362

Scheme 2. Syntheses of PEG^{2000}-Peptidyl-Lipids and PEG^{2000}-Lipid Controls[a]

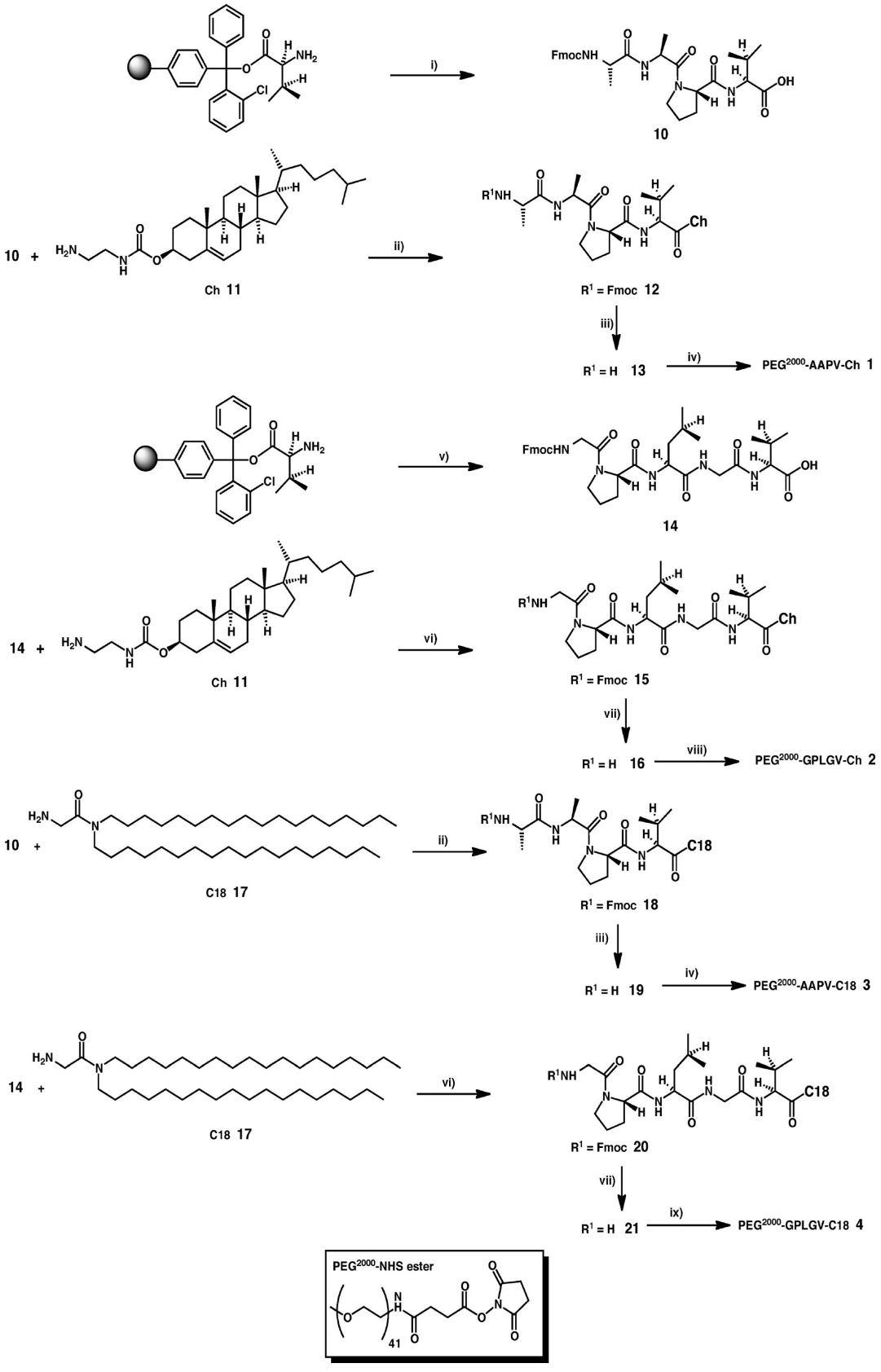

[a](i) (a) Fmoc-Pro-OH (3 equiv), HBTU (2.9 equiv), HOBt (3 equiv), DIPEA (3 equiv), and DMF, 45 min, (b) 20% piperidine, DMF, 10 min (twice), (c) Fmoc-Ala-OH (3 equiv), HBTU (2.9 equiv), HOBt (3 equiv), DIPEA (3 equiv), DMF, 1 h, (d) repeat (b) and (c), (e) 0.5% TFA, CH_2Cl_2, to cleave from the resin, RT, 4 h, 82%; (ii) HBTU (1 equiv), DMAP (3 equiv), dry CH_2Cl_2, overnight, 63−68%; (iii) 20% piperidine. dry CH_2Cl_2, RT, 4 h, 83%; (iv) PEG^{2000}-NHS ester (1 equiv), DIPEA (1 equiv), dry CH_2Cl_2, RT, 18 h, 55%; (v) (a) Fmoc-Gly-OH (3 equiv), HBTU

dx.doi.org/10.1021/bc300419g | Bioconjugate Chem. 2013, 24, 343−362

Scheme 2. continued

(2.9 equiv), HOBt (3 equiv), DIPEA (3 equiv), and DMF, 45 min, (b) 20% piperidine, DMF, 10 min (twice), (c) Fmoc-Leu-OH (3 equiv), HBTU (2.9 equiv), HOBt (3 equiv), DIPEA (3 equiv), DMF, 1 h, (d) repeat (b) and (c) with Fmoc-Pro-OH (3 equiv) and Fmoc-Gly-OH (3 equiv), respectively, in turn, (e) 0.5% TFA, CH_2C1_2, to cleave from the resin, RT, 4 h, 49%; (vi) HBTU (1 equiv), DMAP (3 equiv), dry CH_2Cl_2, overnight, 74%; (vii) 20% piperidine, dry CH_2Cl_2, RT, 4 h, 83%; (viii) PEG^{2000}-NHS ester (1 equiv), DIPEA (1 equiv), dry CH_2Cl_2, RT, 18 h, 47%; (ix) PEG^{2000}-COOH (1 equiv), HBTU (1.2 equiv), DMAP (cat.), dry CH_2Cl_2, RT, 18 h, 25% (overall yield).

in vitro. Our results demonstrate clear boosts to functional delivery in the presence of enzymes that are consistent with the development of enzyme-triggered nanoparticle mediated transfection involving both tumor cell lines. We discuss how the efficiency of enzyme-triggered nanoparticle-mediated transfection could result from partial proteolysis of PEG^{2000}-peptidyl-lipids and the subsequent release or shedding of PEG^{2000}-moieties from nanoparticle surfaces, thereby lowering PEG^{2000}-related inhibitory effects locally and promoting transfection. We also describe an alternative possible mechanism as well. Importantly, functional delivery was achieved using PEGylated pDNA-nanoparticles that have appropriate properties including stability with respect to colloidal aggregation for full in vivo use without further modification.

MATERIALS AND METHODS

General Procedure. Amino acids and resin were purchased from Novabiochem (UK). α-Methoxy-PEG^{2000}-ω-*N*-hydroxysuccinide (PEG^{2000}-NHS ester) was obtained from Rapp Polymere (Tübingen, Germany). Lipids, HLE, MMP-2, and other chemicals used in the synthesis were purchased from Sigma-Aldrich (UK) and were used without further purification. MCF-7 cell lines were purchased from ATCC (LGC, UK). Cell culture medium and other cell culture reagents were obtained from Invitrogen (UK). The compounds were characterized using ^{1}H (400 MHz) NMR and ^{13}C (100 MHz) NMR spectroscopy (Bruker Advance 400). Mass spectroscopy was performed using Bruker Esquire 3000 ESI or VG-070B, Joel SX-102 instruments. High-performance liquid chromatography (HPLC) analysis was conducted on a Hitachi-LaChrom L-7150 pump system connected to a PL-ELS 1000 detector (Polymer Laboratories, UK) using a reverse phase C-4 protein column, gradient mix: 0.0 min [100% A], 15.0−25.0 min [100% B], 25.1−45.0 min [100% C], 45.1−55.0 min [100% A], flow: 1 mL min^{-1}. The cationic lipid *N*′,*N*′-dioctadecyl-*N*-4,8-diaza-10-aminodecanoylglycylamide (DODAG) **7** was prepared as described previously.[22] Dioleoyl-L-α-phosphatidylcholine (DOPC) **8** and cholesterol (Chol) **9** along with all other chemicals were purchased from Sigma-Aldrich, Lancaster, or Merck Biosciences. Full details for the syntheses of PEG^{2000}-peptidyl-lipids **1**−**4** and two PEG^{2000}-lipid controls **5** and **6** are described below (Figure 1; Scheme 2).

Fmoc-AAPV-OH 10. Valyl-2-chlorotrityl resin (500 mg, 0.35 mmol) was added to a solid phase vessel and swelled in dimethylformamide (DMF) (10 mL) and agitated for 2 h. DMF was removed and replaced with a solution of *N*-protected fluorenylmethyloxycarbonyl (Fmoc)-amino acid (1.05 mmol), 2-(1*H*-benzotriazole-1-yl)-1,1,3,3-tetramethyluronium hexafluorophosphate (HBTU) (386.9 mg, 1.02 mmol), hydroxy benzotriazole (HOBt) (141.9 mg, 1.05 mmol), and diisopropylethylamine (DIPEA) (180 μL, 1.05 mmol) in 10 mL DMF. The mixture was agitated for 45 min, then washed twice with DMF and deprotected with 10 mL of 20% (v/v) piperidine in DMF. Cycles of amino acid coupling and Fmoc deprotection were carried out under the same conditions using Fmoc-Pro-OH (354.3 mg, 1.05 mmol) and Fmoc-Ala-OH (326.9 mg, 1.05 mmol), respectively. When the last coupling was achieved, the resin was washed successively with DMF, CH_2Cl_2, MeOH, and Et_2O and allowed to dry under vacuum for 2 h. The peptide was then cleaved off the resin using 10 mL of 0.5% TFA in CH_2Cl_2 for 4 h. The solution was filtered and the solvent was removed in vacuo. The residue was recrystallized in cold Et_2O and the precipitate was freeze−dried overnight to afford the *N*-Fmoc protected-peptide **10** as a white solid (166.4 mg, 82%); ^{1}H NMR (400 MHz, $CDCl_3$) δ_H 0.87, 0.90 (6H, d, J = 6.8 Hz, 2 × CH_3 Val), 1.33, 1.34 (6H, d, J = 6.8 Hz, 2 × CH_3 Ala), 1.93−2.27 (5H, m, CH(β) Val, CH_2(β) Pro, CH_2(γ) Pro), 3.60−3.80 (2H, m, CH_2(δ) Pro), 4.18 (1H, t, J = 7.0 Hz, CH (α) Val), 4.34−4.37 (2H, m, CH (α) Ala), 4.40−4.51 (2H, m, CH (α) Pro, Fmoc CH), 4.60−4.85 (2H, m, Fmoc CH_2), 5.9 (1H, d, J = 7.6 Hz, NH), 7.25−7.77 (8H, Fmoc aromatic CH), 7.93 (1H, NH), 10.61 (1H, COOH); ^{13}C NMR (100 MHz, $CDCl_3$) δ_C 17.3 (2C, 2 × CH_3 Val), 18.5 (2C, 2 × CH_3 Ala), 25.0 (CH_2(γ) Pro), 28.0 (CH_2(β) Pro), 31.2 (CH (β) Val), 37.5 (Fmoc CH), 47.0 (CH (α) Ala), 47.7 (CH_2(δ) Pro), 50.3 (CH (α) Ala), 57.5 (CH(α) Val), 60.4 (CH (α) Pro), 67.5 (Fmoc CH_2), 120.0, 125.1, 127.1, 127.8 (8C, Fmoc aromatic CH), 141.3, 143.7 (4C, Fmoc aromatic C), 156.3 (CO carbamate), 164.2, 171.7, 172.9, 174.2 (4C, CO), 177.0 (COOH); HPLC: R_t = 17.8 min, m/z (ESI +ve) 579 $(M+H)^+$.

***N*^{1}-Cholesteryloxycarbonyl-1,2-diaminoethane 11.** To a stirred solution of ethylene-1,2-diamine (150 mL) at room temperature was added cholesteryl chloroformate (2 g, 4.45 mmol) in $CHCl_3$ dropwise. After 18 h, the reaction was quenched with H_2O (300 mL) and extracted with CH_2Cl_2 (3 × 150 mL). The organic extract was dried over $MgSO_4$ and the solvent was evaporated in vacuo. The compound was purified by flash column chromatography on silica gel (CH_2Cl_2/MeOH/H_2O at 92:7:1 v/v/v) to yield **11** as a white solid (1.71g, 86%); ^{1}H NMR (400 MHz, $CDCl_3$) δ_H 0.66 (3H, s, 18-CH_3), 0.84 (3H, d, J = 6.4 Hz, 27-CH_3), 0.85 (3H, d, J = 6.8 Hz, 26-CH_3), 0.90 (3H, d, J = 6.4 Hz, 21-CH_3), 0.92 (3H, s, 19-CH_3), 1.02−1.63 (21H, m, 1-CH_2, 9-CH, 11-CH_2, 12-CH_2, 14-CH, 15-CH_2, 16-CH_2, 17-CH, 20-CH, 22-CH_2, 23-CH_2, 24-CH_2, 25-CH), 1.76−2.04 (5H, m, 2-CH_2, 7-CH_2, 8-CH), 2.22−2.36 (2H, m, 4-CH_2), 2.79−2.81 (2H, m, 3′-CH_2), 3.19−3.21 (2H, m, 4′-CH_2), 4.52 (1H, m, 3-CH), 5.31 (1H, s, 6-CH); ^{13}C NMR (100 MHz, $CDCl_3$) δ_C 11.8 (18-C),18.6 (21-C), 19.3 (19-C), 21.0 (11-C), 22.5 (26-C), 22.8 (27-C), 23.7 (23-C), 24.2 (15-C), 27.9 (25-C), 28.2 (2C, 2-C, 16-C), 31.8 (2C, 8-C, 7-C), 35.7 (20-C), 36.1 (22-C), 36.5 (10-C), 36.9 (1-C), 38.5 (24-C), 39.4 (4-C), 39.6 (12-C), 39.8 (4′-CH_2), 40.6 (3′-CH_2), 42.2 (13-C), 49.9 (9-C), 56.0 (17-C), 56.6 (14-C), 74.2 (3-C), 122.4 (6-C), 139.8 (5-C), 156.4 (CO carbamate); MS (ESI +ve) 473 $(M + H)^+$, HRMS (FAB +ve) calculated for $C_{30}H_{53}N_2O_2$ (M + H) 473.4119, found 473.4107.

Fmoc-AAPV-(*N*^{1}-cholesteryloxycarbonyl-1,2-diaminoethane) 12. To a solution of *N*-Fmoc-protected peptide **10**

dx.doi.org/10.1021/bc300419g | *Bioconjugate Chem.* 2013, 24, 343−362

(108.6 mg, 0.19 mmol), dimethylaminopyridine (DMAP) (68.6 mg, 0.56 mmol), and HBTU (72.6 mg, 0.19 mmol) in dry $CHCl_3$ (5 mL) was added N^1-cholesteryloxycarbonyl-1,2-diaminoethane **11** (88.2 mg, 0.19 mmol), in dry $CHCl_3$ (3 mL). The mixture was stirred at room temperature under a nitrogen atmosphere for 18 h. Afterward the reaction was quenched with 4% citric acid (4 mL) and washed with $CHCl_3$ (3 × 20 mL). The organic extract was dried over $MgSO_4$, filtered, and concentrated in vacuo to afford the desired *N*-Fmoc-protected peptide−cholesterol conjugate **12** as a pale yellow solid (131.4 mg, 68%); ^{1}H NMR (400 MHz, $CDCl_3$) δ_H 0.66 (3H, s, 18-CH_3), 0.86 (3H, d, J = 6.8 Hz, 27-CH_3), 0.87 (3H, d, J = 6.8 Hz, 26-CH_3), 0.89−1.02 (12H, m, 2 × CH_3 Val, 19-CH_3, 21-CH_3), 1.04−2.38 (41H, m, 2 × CH_3 Ala, CH (β) Val, CH_2 (β) Pro, CH_2 (γ) Pro, 1-CH_2, 2-CH_2, 4-CH_2, 7-CH_2, 8-CH, 9-CH, 11-CH_2, 12-CH_2, 14-CH, 15-CH_2, 16-CH_2, 17-CH, 20-CH, 22-CH_2, 23-CH_2, 24-CH_2, 25-CH, 3′-CH_2), 3.20−3.90 (2H, m, 4′-CH_2), 4.19−4.85 (7H, m, CH (α) Ala, CH (α) Val, CH (α) Pro, Fmoc CH, Fmoc CH_2, 3-CH), 5.32 (1H, s, 6-CH), 7.25−7.76 (8H, Fmoc aromatic CH); ^{13}C NMR (100 MHz, $CDCl_3$) δ_C 11.8 (18-C), 17.7 (2C, 2 × CH_3 Val), 18.5 (2C, 2 × CH_3 Ala), 19.4 (21-C), 21.0 (19-C), 21.3 (11-C), 22.5 (26-C), 22.8 (27-C), 23.0 (CH_2 (γ) Pro), 23.8 (23-C), 24.2 (15-C), 25.1 (CH_2 (β) Pro), 28.0 (25-C), 28.2 (16-C), 28.4 (2-C), 30.1 (CH (β) Val), 31.8 (8-C), 33.6 (7-C), 35.7 (20-C), 36.1 (22-C), 36.5 (10-C), 36.9 (1-C), 38.9 (24-C), 39.5 (2C, 4-C, Fmoc CH), 39.6 (12-C), 39.9 (4′-CH_2), 40.4 (3′-CH_2), 42.2 (13-C), 47.1 (CH (α) Ala), 47.5 (CH_2 (δ) Pro), 47.8 (9-C), 50.2 (CH (α) Ala), 56.1 (17-C), 56.6 (14-C), 57.5 (CH (α) Val), 60.4 (CH (α) Pro), 67.0 (Fmoc CH_2), 74.5 (3-C), 122.5 (6-C), 119.9, 125.1, 127.1, 127.8 (8C, Fmoc aromatic CH), 139.7 (5-C), 142.1, 143.8 (4C, Fmoc aromatic C), 155.8, 156.7 (2C, 2 × CO carbamate), 171.3, 171.5, 172.1, 172.5, (4C, 4 × CO); m/z (ESI +ve) 1033 $(M+H)^+$.

H_2N-AAPV-(N^1-cholesteryloxycarbonyl-1,2-diaminoethane) 13. To a solution of *N*-Fmoc-protected peptide−cholesterol conjugate **12** (97.7 mg, 0.095 mmol) in dry CH_2Cl_2 (4 mL) was added piperidine (1 mL). The reaction was stirred at room temperature under a nitrogen atmosphere for 4 h. The crude mixture was concentrated in vacuo and purified using flash column chromatography (CH_2Cl_2/MeOH/NH_3 [at 92:9:1 v/v/v] to MeOH/CH_2Cl_2 [at 1:2 v/v]) to afford the peptide−cholesterol conjugate **13** as a white solid (63.4 mg, 83%); ^{1}H NMR (400 MHz, $CDCl_3$) δ_H 0.66 (3H, s, 18-CH_3), 0.86 (3H, d, J = 6.8 Hz, 27-CH_3), 0.87 (3H, d, J = 6.8 Hz, 26-CH_3), 0.88−1.03 (12H, m, 2 × CH_3 Val, 19-CH_3, 21-CH_3), 1.07−2.37 (41H, m, 2 × CH_3 Ala, CH (β) Val, CH_2 (β) Pro, CH_2 (γ) Pro, 1-CH_2, 2-CH_2, 4-CH_2, 7-CH_2, 8-CH, 9-CH, 11-CH_2, 12-CH_2, 14-CH, 15-CH_2, 16-CH_2, 17-CH, 20-CH, 22-CH_2, 23-CH_2, 24-CH_2, 25-CH, 3′-CH_2), 3.20−3.85 (2H, m, 4′-CH_2), 4.21−4.80 (4H, m, CH (α) Ala, CH (α) Val, CH (α) Pro, 3-CH), 5.36 (1H, s, 6-CH); ^{13}C NMR (400 MHz, $CDCl_3$) δ_C 11.8 (18-C), 17.4 (2C, 2 × CH_3 Val), 18.6 (2C, 2 × CH_3 Ala), 19.4 (21-C), 21.0 (19-C), 21.5 (11-C), 22.6 (26-C), 22.7 (27-C), 23.0 (CH_2 (γ) Pro), 23.7 (23-C), 24.2 (15-C), 25.2 (CH_2 (β) Pro), 27.9 (25-C), 28.1 (16-C), 28.2 (2-C), 29.8 (CH (β) Val), 31.8 (8-C), 33.6 (7-C), 35.7 (20-C), 36.1 (22-C), 36.5 (10-C), 36.9 (1-C), 38.5 (24-C), 39.4 (4-C), 39.7 (12-C), 40.1 (4′-CH_2), 40.4 (3′-CH_2), 42.2 (13-C), 46.2 (CH (α) Ala), 47.5 (CH_2 (δ) Pro), 47.7 (9-C), 50.2 (CH (α) Ala), 56.1 (17-C), 56.6 (14-C), 58.5 (CH (α) Val), 60.9 (CH (α) Pro), 74.4 (3-C), 122.5 (6-C), 139.7 (5-C), 156.7 (CO carbamate), 171.1, 172.0, 173.1, 175.5, (4C, 4 × CO); m/z (ESI +ve) 811 $(M+H)^+$.

PEG^{2000}-AAPV-(N^1-cholesteryloxycarbonyl-1,2-diaminoethane) 1. To a solution of peptide−cholesterol conjugate **13** (59.2 mg, 0.073 mmol) and DIPEA (12.5 μL, 0.073 mmol) in dry CH_2Cl_2 (5 mL) and under a nitrogen atmosphere was added PEG^{2000}-NHS ester (148.6 mg, 0.073 mmol) in dry CH_2Cl_2 (3 mL). The reaction was stirred at room temperature for 18 h. The solvent was removed in vacuo, and the crude mixture was purified using flash column chromatography (CH_2Cl_2/MeOH/H_2O [at 92:9:1 v/v/v] to MeOH/CH_2Cl_2 [at 1:2 v/v]) to yield the desired PEGylated peptide−cholesterol conjugate **1** as a white solid (109.6 mg, 55%); ^{1}H NMR (400 MHz, $CDCl_3$) δ_H 0.68 (3H, s, 18-CH_3), 0.86 (3H, d, J = 6.8 Hz, 27-CH_3), 0.87 (3H, d, J = 6.8 Hz, 26-CH_3), 0.88−1.03 (12H, m, 2 × CH_3 Val, 19-CH_3, 21-CH_3), 1.06−2.37 (41H, m, 2 × CH_3 Ala, CH (β) Val, CH_2 (β) Pro, CH_2 (γ) Pro, 1-CH_2, 2-CH_2, 4-CH_2, 7-CH_2, 8-CH, 9-CH, 11-CH_2, 12-CH_2, 14-CH, 15-CH_2, 16-CH_2, 17-CH, 20-CH, 22-CH_2, 23-CH_2, 24-CH_2, 25-CH, 3′-CH_2), 3.38 (3H, s, CH_3O), 3.63 (164H, s, PEG CH_2), 3.24−3.85 (2H, m, 4′-CH_2), 4.29−4.74 (4H, m, CH (α) Ala, CH (α) Val, CH (α) Pro, 3-CH), 5.36 (1H, s, 6-CH); ^{13}C NMR (100 MHz, $CDCl_3$) δ_C 11.8 (18-C), 17.3 (2C, 2 × CH_3 Val), 18.6 (2C, 2 × CH_3 Ala), 19.2 (21-C), 19.5 (19-C), 21.0 (11-C), 22.5 (26-C), 22.7 (27-C), 23.0 (CH_2 (γ) Pro), 23.7 (23-C), 24.2 (15-C), 25.2 (CH_2 (β) Pro), 27.9 (25-C), 28.1 (16-C), 28.2 (2-C), 29.8 (CH (β) Val), 31.5 (8-C), 31.7 (7-C), 35.7 (20-C), 36.1 (22-C), 36.5 (10-C), 36.8 (1-C), 38.5 (24-C), 39.4 (4-C), 39.7 (12-C), 40.0 (4′-CH_2), 40.4 (3′-CH_2), 42.2 (13-C), 47.4 (CH (α) Ala), 48.1 (CH_2 (δ) Pro), 48.8 (9-C), 49.9 (CH (α) Ala), 56.1 (17-C), 56.6 (14-C), 58.4 (CH (α) Val), 60.9 (CH (α) Pro), 70.5 (PEG CH_2), 74.3 (3-C), 122.5 (6-C), 139.7 (5-C), 156.6 (CO carbamate), 171.1, 171.5, 172.0, 172.4, 172.6, 173.0 (6C, 6 × CO); HPLC: R_t = 25.6 min, column reverse-phase C-4 protein, gradient mix: 0.0 min [100% A], 15.0−25.0 min [100% B], 25.1−45.0 min [100% C], 45.1−55.0 min [100% A], flow: 1 mL min^{-1}; m/z (MALDI +ve): 2743 $(M+Na)^+$.

Fmoc-GPLGV−OH 14. Synthesized as described in the general procedure for the synthesis of the *N*-Fmoc-protected peptide **10**, using Fmoc-Gly-OH (312.2 mg, 1.05 mmol), Fmoc-Leu-OH (371.1 mg, 1.05 mmol), Fmoc-Pro-OH (354.3 mg, 1.05 mmol), and Fmoc-Gly-OH (312.2 mg, 1.05 mmol), respectively, to afford **14** as a white solid (114 mg, 49%); ^{1}H NMR (400 MHz, $CDCl_3$) δ_H 0.86−0.97 (12H, m, 2 × CH_3 Leu, 2 × CH_3 Val), 1.53−1.85 (3H, m, CH_2 (β) Leu, CH (γ) Leu), 1.98−2.22 (5H, m, CH (β) Val, CH_2 (β) Pro, CH_2 (γ) Pro), 3.5 (2H, m, CH_2 (δ) Pro), 3.61−3.86 (2H, m, CH_2 (α) Gly), 4.0 (2H, s, CH_2 (α) Gly), 4.12−4.27 (4H, m, CH (α) Val, CH (α) Leu, CH (α) Pro, Fmoc CH), 4.30−4.51 (2H, m, Fmoc CH_2), 7.30−7.78 (8H, m, Fmoc aromatic CH); ^{13}C NMR (100 MHz, $CDCl_3$) δ_C 17.8 (2C, 2 × CH_3 Leu), 19.0 (2 × CH_3 Val), 21.6 (CH_2 (β) Leu), 23.0 (CH_2 (γ) Pro), 25.0 (CH_2 (β) Pro), 29.0 (CH (γ) Leu), 30.2 (CH (β) Val), 39.5 (Fmoc CH), 43.0 (CH_2 (α) Gly), 43.6 (CH_2 (α) Gly), 46.9 (CH_2 (δ) Pro), 52.2 (CH (α) Leu), 58.1 (CH (α) Val), 61.2 (CH (α) Pro), 67.3 (Fmoc CH_2), 119.9, 125.1, 127.0, 127.7 (8C, Fmoc aromatic CH), 141.2, 143.7 (4C, Fmoc aromatic C), 157.2 (CO carbamate), 169.9, 170.5, 172.4, 173.4, 173.8 (5C, 5 x CO), 177.5 (COOH); HPLC: R_t = 18.7 min; m/z (ESI +ve) 665 $(M+H)^+$.

Fmoc-GPLGV-(N^1-cholesteryloxycarbonyl-1,2-diaminoethane) 15. Synthesized as described in the general

dx.doi.org/10.1021/bc300419g | *Bioconjugate Chem.* 2013, 24, 343−362

procedure for the *N*-Fmoc-protected peptide−cholesterol conjugate **12**, using *N*-Fmoc-protected peptide **14** (105.0 mg, 0.16 mmol), N^1-cholesteryloxycarbonyl-1,2-diaminoethane **11** (75.6 mg, 0.16 mmol), DMAP (58.6 mg, 0.48 mmol), and HBTU (60.7 mg, 0.16 mmol) to yield **15** as a white solid (132.8 mg, 74%); ^{1}H NMR (400 MHz, $CDCl_3$) δ_H 0.69 (3H, s, 18-CH_3), 0.88 (3H, d, J = 6.8 Hz, 27-CH_3), 0.89 (3H, d, J = 6.8 Hz, 26-CH_3), 0.91−1.01 (18H, m, 2 × CH_3 Leu, 2 × CH_3 Val, 19-CH_3, 21-CH_3), 1.05−2.38 (38H, m, CH_2 (β) Leu, CH (γ) Leu, CH (β) Val, CH_2 (β) Pro, CH_2 (γ) Pro, 1-CH_2, 2-CH_2, 4-CH_2, 7-CH_2, 8-CH, 9-CH, 11-CH_2, 12-CH_2, 14-CH, 15-CH_2, 16-CH_2, 17-CH, 20-CH, 22-CH_2, 23-CH_2, 24-CH_2, 25-CH, 3′-CH_2), 3.25−3.93 (6H, m, CH_2 (γ) Pro, CH_2 (α) Gly, 4′-CH_2), 4.05−4.48 (9H, m, CH_2 (α) Gly, CH (α) Val, CH (α) Leu, CH (α) Pro, Fmoc CH, Fmoc CH_2, 3-CH), 5.34 (1H, s, 6-CH), 7.31−7.78 (8H, m, Fmoc aromatic CH); ^{13}C NMR (100 MHz, $CDCl_3$) δ_C 11.8 (18-C), 17.7 (2 × CH_3 Leu), 18.7 (2 × CH_3 Val), 19.3 (21-C), 21.0 (19-C), 21.3 (11-C), 21.5 (CH_2 (β) Leu), 22.5 (26-C), 22.8 (27-C), 23.0 (CH_2 (γ) Pro), 23.8 (23-C), 24.2 (15-C), 25.1 (CH_2 (β) Pro), 28.0 (25-C), 28.2 (16-C), 29.0 (2-C), 29.4 (CH (γ) Leu), 29.7 (CH (β) Val), 31.8 (2C, 8-C, 7-C), 35.8 (20-C), 36.1 (22-C), 36.5 (10-C), 36.9 (1-C), 38.6 (24-C), 39.5 (2C, 4-C, Fmoc CH), 39.7 (12-C), 39.8 (4′-CH_2), 40.6 (3′-CH_2), 42.3 (13-C), 43.7 (CH_2 (α) Gly), 44.3 (CH_2 (α) Gly), 47.0 (CH_2 (δ) Pro), 49.9 (9-C), 50.0 (CH (α) Leu), 56.1 (17-C), 56.6 (14-C), 59.1 (CH (α) Val), 61.5 (CH (α) Pro), 67.4 (Fmoc CH_2), 74.3 (3-C), 122.5 (6-C), 119.9, 125.0, 127.1, 127.8 (8C, Fmoc aromatic CH), 139.8 (5-C), 141.2, 143.6 (4C, Fmoc aromatic C), 156.7, 157.4 (2C, 2 × CO carbamate), 169.8, 170.5, 172.2, 172.6, 174.7 (5C, 5 × CO); m/z (ESI +ve) 1119 $(M+H)^+$.

H_2N-GPLGV-(N^1-cholesteryloxycarbonyl-1,2-diaminoethane) 16. Synthesized as described in the procedure for the preparation of peptide−cholesterol conjugate **13**, using *N*-Fmoc-protected peptide−cholesterol conjugate **15** (102.9 mg, 0.092 mmol) to afford **16** as a white solid (68.3 mg, 83%); ^{1}H NMR (400 MHz, $CDCl_3$) δ_H 0.74 (3H, s, 18-CH_3), 0.93 (3H, d, J = 6.8 Hz, 27-CH_3), 0.94 (3H, d, J = 6.8 Hz, 26-CH_3), 0.96−1.09 (18H, m, 2 × CH_3 Leu, 2 × CH_3 Val, 19-CH_3, 21-CH_3), 1.13−2.45 (38H, m, CH_2 (β) Leu, CH (γ) Leu, CH (β) Val, CH_2 (β) Pro, CH_2 (γ) Pro, 1-CH_2, 2-CH_2, 4-CH_2, 7-CH_2, 8-CH, 9-CH, 11-CH_2, 12-CH_2, 14-CH, 15-CH_2, 16-CH_2, 17-CH, 20-CH, 22-CH_2, 23-CH_2, 24-CH_2, 25-CH, 3′-CH_2), 3.21−3.95 (6H, m, CH_2 (γ) Pro, CH_2 (α) Gly, 4′-CH_2), 4.10−4.50 (6H, m, CH_2 (α) Gly, CH (α) Val, CH (α) Leu, CH (α) Pro, 3-CH), 5.38 (1H, s, 6-CH); ^{13}C NMR (400 MHz, $CDCl_3$) δ_C 11.8 (18-C), 17.8 (2 × CH_3 Leu), 18.7 (2 × CH_3 Val), 19.3 (21-C), 21.0 (19-C), 21.4 (11-C), 22.6 (CH_2 (β) Leu), 22.7 (26-C), 22.8 (27-C), 23.0 (CH_2 (γ) Pro), 23.8 (23-C), 24.3 (15-C), 25.0 (CH_2 (β) Pro), 28.0 (25-C), 28.2 (16-C), 29.3 (2-C), 29.5 (CH (γ) Leu), 29.7 (CH (β) Val), 31.8 (2C, 8-C, 7-C), 35.8 (20-C), 36.2 (22-C), 36.6 (10-C), 37.0 (1-C), 38.6 (24-C), 39.5 (4-C), 39.7 (12-C), 40.6 (2C, 3′-CH_2, 4′-CH_2), 42.3 (3C, 13C, 2 × CH_2 (α) Gly), 46.6 (CH_2 (δ) Pro), 50.0 (2C, 9-C, CH (α) Leu), 56.1 (17-C), 56.7 (14-C), 58.3 (2C, CH (α) Val, CH (α) Pro), 75.0 (3-C), 122.5 (6-C), 139.8 (5-C), 156.8 (CO carbamate), 169.8, 171.0, 172.4, 172.6, 173.0 (5C, 5 × CO); m/z (ESI +ve) 897 $(M+H)^+$.

PEG^{2000}-GPLGV-(N^1-cholesteryloxycarbonyl-1,2-diaminoethane) 2. Synthesized as described in the procedure for the PEGylated peptide−cholesterol conjugate **1**, using peptide−cholesterol conjugate **16** (68.3 mg, 0.076 mmol), DIPEA (13.1 μL, 0.076 mmol), and PEG^{2000}-NHS ester (155.1 mg, 0.076 mmol) to obtain **2** as a white solid (100 mg, 47%); ^{1}H NMR (400 MHz, $CDCl_3$) δ_H 0.66 (3H, s, 18-CH_3), 0.84 (3H, d, J = 6.8 Hz, 27-CH_3), 0.86 (3H, d, J = 6.8 Hz, 26-CH_3), 0.89−1.02 (18H, m, 2 × CH_3 Leu, 2 × CH_3 Val, 19-CH_3, 21-CH_3), 1.10−2.33 (38H, m, CH_2 (β) Leu, CH (γ) Leu, CH (β) Val, CH_2 (β) Pro, CH_2 (γ) Pro, 1-CH_2, 2-CH_2, 4-CH_2, 7-CH_2, 8-CH, 9-CH, 11-CH_2, 12-CH_2, 14-CH, 15-CH_2, 16-CH_2, 17-CH, 20-CH, 22-CH_2, 23-CH_2, 24-CH_2, 25-CH, 3′-CH_2), 3.38 (3H, s, CH_3O), 3.64 (164H, s, PEG CH_2), 3.20−3.83 (6H, m, CH_2 (γ) Pro, CH_2 (α) Gly, 4′- CH_2), 4.10−4.50 (6H, m, CH_2 (α) Gly, CH (α) Val, CH (α) Leu, CH (α) Pro, 3-CH), 5.34 (1H, s, 6-CH); ^{13}C NMR (100 MHz, $CDCl_3$) δ_C 11.8 (18-C), 17.8 (2C, 2 × CH_3 Leu), 18.7 (2C, 2 × CH_3 Val), 19.3 (21-C), 21.0 (19-C), 21.3 (11-C), 22.5 (CH_2 (β) Leu), 22.8 (26-C), 23.0 (27-C), 23.2 (CH_2 (γ) Pro), 23.8 (23-C), 24.3 (15-C), 25.0 (CH_2 (β) Pro), 28.0 (25-C), 28.2 (16-C), 28.9 (2-C), 29.6 (CH (γ) Leu), 30.3 (CH (β) Val), 31.8 (2C, 8-C, 7-C), 35.8 (20-C), 36.1 (22-C), 36.5 (10-C), 37.0 (1-C), 38.6 (24-C), 39.5 (4-C), 39.7 (12-C), 40.0 (2C, 3′-CH_2, 4′-CH_2), 42.3 (3C, 13C, 2 × CH_2 (α) Gly), 47.5 (CH_2 (δ) Pro), 50.0 (2C, 9-C, CH (α) Leu), 56.1 (17-C), 56.6 (14-C), 59.0 (3C, CH (α) Val, CH (α) Pro, CH_3O), 70.5 (PEG CH_2), 74.2 (3-C), 122.4 (6-C), 139.8 (5-C), 156.6 (CO carbamate), 169.4, 170.5, 172.0, 172.5, 173.0, 173.3, 174.2 (7C, 7 × CO); HPLC: R_t = 25.5 min, column reverse-phase C-4 protein, gradient mix: 0.0 min [100% A], 15.0−25.0 min [100% B], 25.1−45.0 min [100% C], 45.1−55.0 min [100% A], flow: 1 mL min^{-1}; m/z (MALDI +ve): 2829 $(M+Na)^+$.

N^2-PEG^{2000}-(N^1-cholesteryloxycarbonyl-1,2-diaminoethane) 5. To a stirred solution of N^1-cholesteryloxycarbonyl-1,2-diaminoethane **11** (60 mg, 0.127 mmol) and DIPEA (21.8 μL, 0.127 mmol) in dry CH_2Cl_2 (5 mL) at room temperature and under a nitrogen atmosphere was added PEG^{2000}-NHS ester (258.5 mg, 0.127 mmol) in dry CH_2Cl_2 (3 mL). After 18 h, the crude mixture was concentrated in vacuo and recrystallized in cold Et_2O to afford **5** as a white solid (298 mg, 98%); ^{1}H NMR (400 MHz, $CDCl_3$) δ_H 0.68 (3H, s, 18-CH_3), 0.86 (3H, d, J = 6.4 Hz, 27-CH_3), 0.87 (3H, d, J = 6.4 Hz, 26-CH_3), 0.91 (3H, d, J = 6.4 Hz, 21-CH_3), 1.00 (3H, s, 19-CH_3), 1.05−1.62 (21H, m, 1-CH_2, 9-CH, 11-CH_2, 12-CH_2, 14-CH, 15-CH_2, 16-CH_2, 17-CH, 20-CH, 22-CH_2, 23-CH_2, 24-CH_2, 25-CH), 1.78−2.04 (5H, m, 2-CH_2, 7-CH_2, 8-CH), 2.06−2.15 (2H, m, 4-CH_2), 2.25−2.38 (2H, m, 3′-CH_2), 3.25−3.35 (2H, m, 4′-CH_2), 3.38 (3H, s, CH_3O), 3.64 (164H, s, PEG CH_2), 4.48 (1H, m, 3-CH), 5.36 (1H, s, 6-CH); ^{13}C NMR (100 MHz, $CDCl_3$) δ_C 11.8 (18-C), 18.7 (21-C), 19.3 (19-C), 21.1 (11-C), 22.5 (26-C), 22.8 (27-C), 23.8 (23-C), 24.2 (15-C), 28.0 (25-C), 28.2 (2C, 2-C, 16-C), 31.8 (2C, 8-C, 7-C), 35.7 (20-C), 36.1 (22-C), 36.5 (10-C), 37.0 (1-C), 38.6 (24-C), 39.5 (4-C), 39.7 (12-C), 41.0 (2C, 3′-CH_2, 4′-CH_2), 42.3 (13-C), 50.0 (9-C), 56.1 (17-C), 56.6 (14-C), 59.0 (CH_3O), 70.5 (PEG CH_2), 74.2 (3-C), 122.4 (6-C), 139.8 (5-C), 170.8, 172.4 (2C, 2 x CO); HPLC: R_t = 25.5 min, column reverse phase C-4 protein, gradient mix: 0.0 min [100% A], 15.0−25.0 min [100% B], 25.1−45.0 min [100% C], 45.1−55.0 min [100% A], flow: 1 mL min^{-1}; m/z (MALDI +ve): 2405 $(M+Na)^+$.

***N*′-PEG^{2000}-AAPV-*N,N*-dioctadecylglycylamide 3.** *N,N*-Dioctadecylglycylamide **17** was prepared as described previously,[22] and coupled to Fmoc-AAPV-OH **10** (in the same way as described for **12** above) to give Fmoc-AAPV-*N,N*-dioctadecylglycylamide **18** that was immediately Fmoc deprotected to give **19** (as for **13** above), then coupled to

dx.doi.org/10.1021/bc300419g | *Bioconjugate Chem.* 2013, 24, 343−362

PEG^{2000}-NHS ester in the same was as described for **1**, giving *N′*-PEG^{2000}-AAPV-*N,N*-dioctadecylglycylamide **3** in decent overall yield (75 mg, 25%); ^{1}H NMR (400 MHz, $CDCl_3$) δ_H 0.88−0.94 (18H, m, CH_3, *N*-dioctadecylamine, 2 × CH_3 Val, 2 × CH_3 Ala), 1.19−1.38 (60H, m, CH_2 (*N*-dioctadecylamine)), 1.43−1.59 (4H, m, CH_2 (*N*-dioctadecylamine)), 1.96−2.31 (4H, m, CH_2 (β) Pro, CH_2 (γ) Pro), 2.54−2.61 (5H, m, CH_2 PEG, CH (β) Val), 3.13−3.15 (2H, tr, CH_2 (*N*-dioctadecylamine)), 3.28−3.32 (2H, tr, CH_2 (*N*-dioctadecylamine)), 3.42−3.46 (4H, m, CH_2, (δ) Pro, (α) Gly), 3.38 (3H, s, CH_3O), 3.63 (164H, br s, PEG CH_2), 4.29−4.74 (4H, m, 2 × CH (α) Ala, CH (α) Val, CH (α) Pro); ^{13}C NMR (100 MHz, $CDCl_3$) δ_C 11.8 (Me, octadecyl), 17.3 (2C, 2 × CH_3 Val), 18.6 (2C, 2 × CH_3 Ala), 19.3, 21.0, 21.3, 22.8, 23.0 (CH_2, octadecyl), 23.2 (CH_2 (γ) Pro), 23.8, 24.3 (CH_2, octadecyl), 25.2 (CH_2 (β) Pro), 28.0, 28.2, 28.9 (CH_2, octadecyl), 29.8 (CH (β) Val), 31.8, 35.8, 36.1, 36.5, 37.0, 38.6, 39.5, 39.7, 40.0, 42.3 (3C, 2 × NCH_2R, CH_2 (α) Gly), 47.4 (CH, (α) Ala), 47.5 (CH (α) Pro), 48.1 (CH_2 (δ) Pro), 49.9 (CH (α) Ala), 56.1, 56.6 (CH_2), 58.4 (CH (α) Val), 60.9 (CH_3O-PEG), 70.5 (PEG CH_2), 170.5, 172.0, 172.5, 173.0, 173.3, 174.2 (6C, 6 × CO); HPLC: R_t = 25.4 min, column reverse phase C-4 protein, gradient mix: 0.0 min [100% A], 15.0−25.0 min [100% B], 25.1−45.0 min [100% C], 45.1−55.0 min [100% A], flow: 1 mL min^{-1}; *m*/*z* (MALDI +ve): 2849 (M+Na)$^+$.

***N′*-PEG^{2000}-GPLGV- *N,N*-dioctadecylglycylamide 4.** *N,N*-Dioctadecylglycylamide **17** was prepared as described previously,[22] and coupled to Fmoc-GPLGV-OH **14** (in the same way as described for **15** above) to give Fmoc-GPLGV-*N,N*-dioctadecylglycylamide **20** that was immediately Fmoc deprotected to give the conjugate H_2N-GPLGV-*N,N*-dioctadecylglycylamide **21** (as for **16** above). Conjugate **21** (100 mg, 0.1 mmol) was then dissolved in CH_2Cl_2, and HBTU (379.3 mg, 0.12 mmol) with DMAP (cat) added gradually in CH_2Cl_2 solution. The mixture was left stirring for 30 min. PEG^{2000}-COOH (199 mg, 0.1 mmol) dissolved in CH_2Cl_2 was added slowly and the whole was left stirring overnight at room temperature giving *N′*-PEG^{2000}-GPLGV-*N,N*-dioctadecylglycylamide **4** as a white−yellow solid (75 mg, 25%) after purification by flash chromatography (hexane and mixture hexane:ethyl acetate); ^{1}H NMR (400 MHz, $CDCl_3$) δ_H 0.88−0.94 (18H, m, 6 × CH_3 (*N*-dioctadecylamine, Leu, Val)), 1.19−1.38 (60H, m, CH_2 (*N*-dioctadecylamine)), 1.43−1.59 (5H, m, 2 × CH_2 (*N*-dioctadecylamine), CH (γ) Leu), 1.81−2.19 (2H, m, CH_2 (β) Leu), 1.96−2.31 (4H, m, CH_2 (β) Pro, CH_2 (γ) Pro), 2.54−2.61 (5H, m, CH_2 PEG, CH (β) Val), 3.14 (2H, tr, CH_2 (*N*-dioctadecylamine)), 3.30 (2H, tr, CH_2 (*N*-dioctadecylamine)), 3.42−3.46 (4H, m, CH_2, (δ) Pro, (α) Gly), 3.38 (3H, s, CH_3O), 3.55−3.72 (164H, m, 82 × CH_2 PEG, CH_2 PEG), 3.99−4.12 (4H, m, CH_2 (α) Gly, CH_2 (α) Gly), 4.31−4.35 (1H, m, CH (α) Val), 4.57−4.61 (1H, m, CH (α) Leu); ^{13}C NMR (100 MHz, $CDCl_3$) δ_C 11.8 (Me, octadecyl), 17.8 (2C, 2 × CH_3 Leu), 18.7 (2C, 2 × CH_3 Val), 19.3, 21.0, 21.3 (CH_2, octadecyl), 22.5 (CH_2 (β) Leu), 22.8, 23.0 (CH_2 octadecyl), 23.2 (CH_2 (γ) Pro), 23.8, 24.3 (CH_2 octadecyl), 25.0 (CH_2 (β) Pro), 28.0, 28.2, 28.9 (CH_2 octadecyl), 29.6 (CH (γ) Leu), 30.3 (CH (β) Val), 31.8, 35.8, 36.1, 36.5, 37.0, 38.6, 39.5, 39.7, 40.0, 42.3 (5C, 2 × NCH_2R, 3 × CH_2 (α) Gly), 47.5 (CH (α) Pro), 48.1 (CH_2 (δ) Pro), 50.0 (CH (α) Leu), 56.1, 56.6, 59.0 (2C, CH (α) Val, CH_3O-PEG), 70.5 (PEG CH_2), 169.4, 170.5, 172.0, 172.5, 173.0, 173.3, 174.2 (7C, 7 × CO); HPLC: R_t = 25.5 min, column reverse phase C-4 protein, gradient mix: 0.0 min [100% A], 15.0−25.0 min [100% B], 25.1−45.0 min [100% C], 45.1−55.0 min [100% A], flow: 1 mL min^{-1}; *m*/*z* (MALDI +ve): 2935 (M+Na)$^+$.

***N′*-PEG^{2000}-*N,N*-dioctadecylglycylamide 6.** To a stirred solution of *N,N*-dioctadecylglycylamide **17** (60 mg, 0.127 mmol) and DIPEA (21.8 μL, 0.127 mmol) in dry CH_2Cl_2 (5 mL) at room temperature and under a nitrogen atmosphere was added PEG^{2000}-NHS ester (258.5 mg, 0.127 mmol) in dry CH_2Cl_2 (3 mL). After 18 h, the crude mixture was concentrated in vacuo and recrystallized in cold Et_2O to afford the final product **6** as a white solid (298 mg, 98%); ^{1}H NMR (400 MHz, $CDCl_3$) δ_H 0.88−0.94 (6H, m, 2 × CH_3 (*N*-dioctadecylamine)), 1.19−1.38 (60H, m, CH_2 (*N*-dioctadecylamine)), 1.43−1.59 (4H, m, 2 × CH_2 (*N*-dioctadeyclamine)), 2.54−2.61 (4H, m, CH_2 PEG), 3.14 (2H, tr, CH_2 (*N*-dioctadecylamine)), 3.30 (2H, tr, CH_2 (*N*-dioctadecylamine)), 3.42−3.46 (2H, m, CH_2 (α) Gly), 3.38 (3H, s, CH_3O), 3.55−3.72 (164H, m, 82 × CH_2 PEG, CH_2 PEG); ^{13}C NMR (100 MHz, $CDCl_3$) δ_C 11.8 (Me, octadecyl), 19.3, 21.0, 21.3, 22.8, 23.0, 23.8, 24.3, 25.0, 28.0, 28.2, 28.9, 31.8, 35.8, 36.1, 36.5, 37.0, 38.6 (CH_2, octadecyl), 39.5, 39.7, 40.0, 42.3 (3C, 2 × NCH_2R, CH_2 (α) Gly), 56.1, 56.6, 59.0 (CH_3O-PEG), 70.5 (PEG CH_2), 170.8, 172.4 (2C, 2 × CO); HPLC: R_t = 25.5 min, column reverse phase C-4 protein, gradient mix: 0.0 min [100% A], 15.0−25.0 min [100% B], 25.1−45.0 min [100% C], 45.1−55.0 min [100% A], flow: 1 mL min^{-1}; *m*/*z* (MALDI +ve): 2511 (M+Na)$^+$.

Preparation of pDNA. Transformed *E. coli* containing pEGFPLuc (pDNA, 6.4 kb) was grown in sterilized LB medium (5 mL) with kanamycin (5 μL) overnight at 37 °C with shaking. Next day, the culture was transferred to sterilized LB medium (500 mL) with kanamycin (500 μL) and was grown at 37 °C with shaking overnight. Isolation of pDNA was carried out using E.Z.N.A. Endo-Free Plasmid Kit (Omega Bio-Tek) for preparation of plasmid with low endotoxin levels. pDNA concentration was determined using Nanodrop ND-1000 (Thermo Fisher Scientific, MA, USA), and found to be 0.5−0.6 μg/μL. The pDNA quality was assessed by agarose gel electrophoresis.

Preparation of pDNA Nanoparticles. DODAG **7**, DOPC **8**, cholesterol **9**, and the PEG^{2000}-lipids **1**−**6** were prepared as stock solutions in $CHCl_3$ and stored at −20 °C. Appropriate volumes of each lipid stock were combined in a round-bottom flask (5 mL) containing $CHCl_3$ (500 μL). The solvent was slowly removed in vacuo to form an even lipid film that was then purged with N_2 (g) to remove residual traces of organic solvent. The film was rehydrated with 4 mM (2-[4-(2-hydroxyethyl)piperazin-1-yl]ethanesulfonic acid) HEPES (pH 7.0) to obtain a total lipid concentration of 1 mg/mL. Lipid suspensions were subsequently subjected to sonication at 40 °C for 40 min, leading to the formation of uniform, unilamellar PEGylated cationic liposomes (see Tables 1 and 2). PEGylated pDNA nanoparticles were then prepared by mixing the appropriate volume of pDNA with the resulting liposome solutions under heavy vortex mixing conditions to obtain nanoparticles at the desired lipid/pDNA ratio (typically 12:1 w/w).

Determination of pDNA Entrapment Efficiencies and Nanoparticle Stabilities. *Propidium Iodide (PI) Assay.* PEGylated pDNA nanoparticles were prepared, as described previously, at lipid/pDNA ratios of 1:1, 2:1, 4:1, 8:1, 12:1, and 16:1 w/w. After 10 min incubation at ambient temperature, the nanoparticles were diluted in 4 mM HEPES buffer, pH 7.0

Table 1. Summary of "Higher Charged" CLI and BC1 Family Cationic Liposomes

	mol %			
lipid	**CL 1**	**BC1**		
PEG^{2000}-peptidyl lipids:				
PEG^{2000}-AAPV-Ch **1**		1 or 5		
PEG^{2000}-GPLGV-Ch **2**			1 or 5	
PEG^{2000}-lipids:				
PEG^{2000}-Ch **5**				1 or 5
DODAG **7**	50	50	50	50
DOPC **8**	20	19 or 15	19 or 15	19 or 15
Cholesterol **9**	30	30	30	30

(total final volume 100 μL). PI solution (100 μL, 2.5 μM) was added and the mixtures were incubated at 37 °C for 5 min. The fluorescence intensity (A_{ex} 535 nm, I_{em} 617 nm) of each mixture was measured at using a Varioskan flash microplate reader. The fluorescence intensities of PEGylated liposomes alone in PI solution (with no pDNA present) and of PI solution alone were subtracted as background measurements. The percentage of pDNA entrapment ($\%_{en\text{-}pDNA}$) follows eq 1

$$\%_{en-pDNA} = 100 \times [1 - (I_{pDNA-NPs}/I_{pDNA})] \quad (1)$$

where $I_{pDNA\text{-}NPs}$ represents the measured fluorescence intensity of a given solution of nanoparticle complexed pDNA incubated with PI solution, and I_{pDNA} the measured fluorescence intensity of a corresponding concentration matched control solution of free pDNA also incubated with PI solution.

Agarose Gel Electrophoresis. PEGylated pDNA nanoparticles were prepared as described previously at 1:1, 2:1, 4:1, 8:1, and 12:1 lipid/pDNA w/w. After 10 min incubation at ambient temperature, the nanoparticles were diluted in 4 mM HEPES, pH 7 buffer, to a total volume of 50 μL. Nanoparticle suspensions (20 μL, 0.4 μg pDNA/well) were combined with 6× orange DNA loading dye (1 μL) and then loaded into individual wells of 0.8% agarose gels. The DNA molecular weight marker used in each gel was GeneRuler Ladder mix (Thermo Fisher Scientific). Gel electrophoresis was performed at +65 mV for 3 h and gels were visualized under UV light.

Size and Zeta Potential Measurements. Sizes of all cationic liposomes, pDNA lipoplex nanoparticles, and PEGylated pDNA nanoparticles were measured by dynamic light scattering using a Delta N4+ 440SX particle analyzer (Coulter). Scattering was detected at 25 °C using a 90° scattering angle. Mean nanoparticle diameters were determined by calculation from unimodal size distributions. The zeta potential measurements were performed on a Nanoseries Nano-ZS zetasizer (Malvern, UK) equipped with a 4 mW He−Ne laser (633 nm) and avalanche photodiode detector. All samples were prepared in 4 mM HEPES buffer, pH 7 (total lipid concentration 0.5 mg/mL).

Nanoparticle Stability Assays. pDNA lipoplex nanoparticles and PEGylated pDNA nanoparticles were prepared at lipid/pDNA ratio of 12:1 w/w, as described previously. Aliquots of nanoparticles (containing 1 μg pDNA) were diluted with complete media (500 μL) comprising 10% fetal calf serum (FCS). The particles sizes were recorded immediately using dynamic light scattering. The mixtures were incubated at 37 °C and nanoparticle diameters were measured at 30 min intervals over 4 h. In the case of 80% FCS stability measurements, aliquots of FCS (400 μL) were added to the nanoparticle solutions (100 μL, containing 1 μg pDNA) and the absorbance of the mixtures was recorded immediately at 600 nm using an UV spectrometer. The mixtures were incubated at 37 °C and their absorbance was measured at 30 min intervals over 4 h.

pDNA-Nanoparticles Transfection Efficiencies. *MCF-7 Cell Line Transfections in Vitro.* MCF-7 cells were seeded at 6 × 10^4 per well in 24-well plates, then grown in Dulbecco's Modified Eagle's Medium (DMEM) supplemented with 10% FCS, 1% penicillin, and streptomycin (500 μL of complete medium), at 37 °C in a humidified, 5% CO_2 atmosphere for 72 h prior to the assay (until 80% confluent). The media was then removed and replaced with fresh media containing either **AB1** or **AB2** lipoplex nanoparticles or 1 or 5 mol % PEGylated pDNA-**ABC1** or **ABC2** nanoparticles (Tables 1 and 2). All nanoparticles were prepared with a lipid/pDNA ratio of 12:1 w/w. HLE (10 μL, 1.03 μM) was added to the first set and incubated at room temperature for 10 min, while the other set contained no HLE. After mixtures were added to each well (1 μg pDNA per well), plates were then incubated at 37 °C in 5% CO_2 atmosphere for 6 h. Following this in each well, media was removed, cells were washed with phosphate-buffered saline (PBS) (2 × 500 μL), and then fresh media was added (500 μL). After further incubation at 37 °C for 24 h, the cells in each well were washed with PBS (2 × 500 μL) and 1× cell culture lysis reagent (80 μL) was added. One freeze−thaw cycle was carried out to ensure the complete lysis. Cells were then scraped from each well, and the lysates were centrifuged (5000 rpm, 2 min) to separate cellular debris. The supernatants were then analyzed for luciferase gene expression using a luciferase assay system (Promega, USA), performed on a Berthold Lumat

Table 2. Summary of "Lower Charged" CL2 and BC2 Family Cationic Liposomes

	mol %						
lipid	**CL 2**	**BC2** family					
PEG^{2000}-peptidyl lipids:							
PEG^{2000}-AAPV-Ch **1**		1 or 5					
PEG^{2000}-GPLGV-Ch **2**			1 or 5				
PEG^{2000}-AAPV-C18 **3**					1 or 5		
PEG^{2000}-GPLGV-C18 **4**						1 or 5	
PEG^{2000}-lipids:							
PEG^{2000}-Ch **5**				1 or 5			
PEG^{2000}-C18 **6**							1 or 5
DODAG **7**	20	20	20	20	20	20	20
DOPC **8**	50	49 or 45	49 or 45	49 or 45	49 or 45	49 or 45	49 or 45
Chol **9**	30	30	30	30	30	30	30

dx.doi.org/10.1021/bc300419g | *Bioconjugate Chem.* 2013, 24, 343−362

LB 9507 luminometer. Transfection efficiencies were measured in relative light units (RLU) and normalized to total protein content determined with bicinchoninic acid (BCA) protein assay kit (Pierce, Thermo Scientific). The data were reported as RLU/mg protein.

HT1080 Cell Line Transfections in Vitro. HT1080 cells were seeded in a 24-well plate (5.0×10^4 cells per well) then grown in DMEM supplemented with 10% FCS, 1% penicillin and streptomycin (complete medium), at 37 °C in a humidified, 5% CO_2 atmosphere for 24 h prior to the assay (until 60% confluent). The media was then removed and replaced with fresh media containing either **AB1** or **AB2** lipoplex nanoparticles or 1 or 5 mol % PEGylated pDNA-**ABC1** or **ABC2** nanoparticles (see Tables 1 and 2). All nanoparticles were prepared with a lipid/pDNA ratio of 12:1 w/w. Cells were then incubated at 37 °C in 5% CO_2 atmosphere for 24 h. After media was removed, cells in each well were washed with PBS (2 × 500 μL), and fresh media was added (500 μL). Then cells were incubated for a further 24 h before luciferase assays were carried out. In order to measure MMP-2 levels, HT1080 cells were grown to 60% confluence (as above), then for a further 24 h at 37 °C with 5% CO_2. Cell supernatants were collected and centrifuged (50 000*g* for 2 min) to separate out cellular debris. Thereafter, the determination of MMP-2 levels in cell supernatants were carried out using MMP-2 human Elisa assay kit (Life Science Technologies).

Fluorescence Microscopy of pDNA Nanoparticle-Mediated Transfection. *MCF-7 Cell Line Transfections in Vitro.* MCF-7 cells were seeded in a 6-well plate (1.2×10^5 cells per well, 2 mL) containing microscope coverslips (1 mm, thickness) for 72 h prior to fluorescent labeling. The cells were grown until 80% confluent at 37 °C in a humidified, 5% CO_2 atmosphere. The media was then removed and replaced with fresh media containing either 1 or 5 mol % PEGylated pDNA-**ABC2** nanoparticles (formulated using the following PEG-lipids: PEG^{2000}-AAPV-Ch **1**, PEG^{2000}-AAPV-C18 **3**, PEG^{2000}-Ch **5**, or PEG^{2000}-C18 **6**) (see Tables 1 and 2) (48 μg/well of total lipid). All nanoparticles were also labeled with 1 mol % dioleoyl-L-α-phosphatidylethanolamine-*N*-(lissamine rhodamine B sulphonyl) (DOPE-Rhoda) with a lipid/pDNA ratio of 12:1 w/w. HLE (10 μL, 1.03 μM) was added as appropriate, then plates were incubated at 37 °C in 5% CO_2 atmosphere for 6 h. Media was then removed, and cells washed with PBS (2 × 2 mL). Then cells were treated with paraformaldehyde (1 mL, 4% v/v) and incubated at 37 °C for 20 min. Next cells were then washed with PBS (2 × 2 mL) and incubated with glycine solution (1 mL, 20 mg mL^{-1}) at 37 °C for 20 min. Thereafter cells were washed with PBS (2 × 2 mL) and stained with 4′,6-diamidino-2-phenylindole (DAPI) (1 mL, 100 nM) at 37 °C for 5 min. The cells were washed with PBS (2 × 2 mL) one final time, then the coverslips were removed from the wells and mounted face-down on microscope slides using PBS: glycerol (10 μL, 1:1 v/v). Microscopy images were obtained on a Eclipse E600 microscope (Nikon).

HT1080 Cell Line Transfections in Vitro. HT1080 cells were seeded in 6-well plates (8×10^4 cells per well, 2 mL) containing microscope coverslips for 24 h prior to fluorescent labeling. The cells were grown until 60% confluent at 37 °C in a humidified, 5% CO_2 incubator. The media was then removed and replaced with fresh media containing 1 or 5 mol % PEGylated pDNA-**ABC2** nanoparticles (formulated using the following PEG-lipids: PEG^{2000}-GPLGV-Ch **2**, PEG^{2000}-GPLGV-C18 **4**, PEG^{2000}-Ch **5**, or PEG^{2000}-C18 **6**) (48 μg/well of total lipid). All nanoparticles were also labeled with 1 mol % DOPE-Rhoda and with a lipid/pDNA ratio of 12:1 w/w. Plates were incubated at 37 °C in 5% CO_2 atmosphere for 24 h. Following this, coverslips were fixed and mounted as described above. Microscopy images were taken on an Olympus 251 scope, and confocal images were obtained using an upright Leica Confocal Microscope.

RESULTS AND DISCUSSION

Syntheses of PEG^{2000}-Peptidyl-Lipids. We prepared two classes of PEG^{2000}-peptidyl lipids enabled for elastase and MMP-2 mediated enzymatic dePEGylation (Figure 1; Scheme 2). Two PEG^{2000}-peptidyl lipids **1** and **2** were prepared from N^1-cholesteryloxycarbonyl-1 2-diaminoethane (Ch) **11**; two alternative PEG^{2000}-peptidyl lipids **3** and **4** were prepared from *N,N*-dioctadecylglycylamide (C18) **17**. Of these, PEG^{2000}-peptidyl lipids **1** and **3** were constructed with the peptide hydrolysis consensus sequences for elastase, namely, Ala.Ala.Pro.Val (AAPV).[13] PEG^{2000}-peptidyl lipids **2** and **4** were constructed with the corresponding hydrolysis consensus sequence for MMP-2 given as Gly.Pro.Leu.Gly.Val (GPLGV).[23]

For PEG^{2000}-peptidyl lipids **1** and **3**, Fmoc-AAPV-OH **10** was obtained first from solid-phase peptide synthesis (SPPS), then amide coupled to lipid moieties **11** or **17** yielding Fmoc-AAPV-lipids **12** or **18**, respectively. Fmoc deprotection was then performed in 20% piperidine for 4 h. Afterward, NH_2-AAPV-lipids **13** or **19** were amide-conjugated with PEG^{2000}-NHS ester in the presence of DIPEA to give **1** and **3** in good overall yield. Analytical HPLC was used to monitor coupling reactions. For PEG^{2000}-peptidyl lipids **2** and **4**, Fmoc-GPLGV-OH **14** was obtained from SPPS again, then amide coupled directly to lipid moieties **11** or **17** yielding Fmoc-GPLGV-lipids **15** or **20**, respectively. Fmoc deprotection was effected as above then NH_2-GPLGV-lipid **16** was amide-conjugated with PEG^{2000}-NHS ester in the presence of base, DIPEA to give **2** in good overall yield. Alternatively, NH_2-GPLGV-lipid **21** was amide-conjugated with PEG^{2000}-COOH acid in the presence of HBTU and DMAP to give **4** in decent overall yield. Coupling reactions were monitored by analytical HPLC. Finally, two different control PEG^{2000}-lipids **5** or **6** were also prepared by amide coupling of PEG^{2000}-NHS ester to lipid moieties **11** or **17**, respectively, avoiding the inclusion of central peptide hydrolysis consensus sequences for control experiment purposes (Figure 1).

Nanoparticle Preparation. Nucleic acid containing nanoparticles were then constructed from families of PEGylated cationic liposomes. Throughout, the cationic lipid employed was the recently described DODAG **7**.[22] The other neutral lipids used in the formulation of our PEGylated cationic liposome formulations are shown (Figure 1). This selection of lipids used was made with an eye to potential direct translation of nanoparticles under investigation into in vivo studies based upon previous knowledge. Therefore, the following two main points were taken into consideration: (1) There is general agreement that protonated functional groups in a cationic lipid polar headgroup promote both nucleic acid association and cellular uptake/internalization via electrostatic interactions with anionic cell surfaces. However, although a cationic headgroup is critical for functional nucleic acid delivery, cationic liposomes formulated using a high mol % (at least 50 mol %) of cationic lipid can be associated with increased risk of cellular toxicity.[24,25] (2) In a lipid-based nanoparticle formulation, the cationic lipid is frequently paired with a fusogenic lipid, (e.g.,

dioleoyl-L-α-phosphatidylethanolamine [DOPE]). Such a fusogenic lipid is considered to assist the process of functional nucleic acid delivery by promoting the endosomolysis step that follows nanoparticle cell entry by endocytosis, in order for associated nucleic acids to enter cell cytoplasm. Endosomolysis appears to be promoted by membrane fusion involving the bilayer membranes of internalized nanoparticles and surrounding endosome bilayer membranes. Fusogenic lipids favor the adoption of hexagonal (H_I and H_{II}) fluid mesophases between adjacent bilayer membranes that make membrane fusion possible.[26,27] Unfortunately, the inclusion of fusogenic lipids can have a negative impact on nanoparticle stability in vivo biological fluids leading to nanoparticle aggregation and loss of delivery function.[28,29]

Considering the first point above, DODAG **7** is thought to possess a conical molecular shape that can be incorporated into typical bilayer membranes but favors hexagonal H_I fluid mesophase formation.[22] This particular molecular shape has recently assisted and enabled us to employ DODAG **7** cationic lipids in the formulation of a range of "lower charged" cationic liposome and corresponding nucleic acid-nanoparticle formulations with as low as 10−15 mol % DODAG **7** (data not shown).

Considering the second point above, DODAG **7** possesses three amine functional groups but actually is reasoned to present a net charge of 1.7 at neutral pH due to downward perturbations in pK_a values of amine functional groups in the polar headgroup separated by short ethylene group spacings.[22] Such unprotonated amine functional groups at neutral pH should have the capacity to become protonated during the process of endosome compartment acidification, post-endocytosis of nanoparticles, thereby inducing a rise in intracompartment ionic strength that could lead to endosomolysis by osmotic shock,[30] or by multivalent ionic interactions with anionic endosomal membranes that become unstable through the exclusion of surface water molecules. Moreover, the conical molecular shape of DODAG **7**, as discussed above, ensures that this cationic lipid possesses potential membrane fusogenic properties that could synergize with its osmotic shock-promoting properties in aiding endosomolysis.

Accordingly, since DODAG **7** appears to have favorable charge and shape characteristics for low mol % formulations, and shape characteristics that might promote membrane fusogenicity, then our approach to lipid-based nanoparticle formulations in this case was to concentrate on balancing the use of DODAG **7** with more stabilizing lipids such DOPC **8** and cholesterol **9**. DOPC **8** has a cylindrical molecular shape that favors bilayer formation and appears to promote the formation of small (approx 100 nm diameter) stable nanoparticles with properties appropriate for stability in biological fluids including long-term (>6 h) systemic circulation.[31] In a similar vein, cholesterol **9** is considered to increase nanoparticle stabilities due to its ability to decrease membrane permeability and prevent plasma protein adsorption.[32,33] Gratifyingly, replacement of DOPE with cholesterol **9** has been shown previously as well to promote actual increases in levels of gene expression in vivo.[28,34,35] In addition, we chose to combine DOPC **8** and cholesterol **9** together with synthetic PEG^{2000}-peptidyl lipids **1**, **2**, **3**, or **4** (or the PEG^{2000}-lipids **5** or **6** where applicable) in order to prepare appropriate PEGylated cationic liposomes and corresponding pDNA-nanoparticles for our studies reported below.

Physical Properties of "Higher Charged" pDNA-Nanoparticles. Initially, our first studies were performed with "higher charged" cationic liposomes **CL1**, prepared using 50 mol % of DODAG **7** (Table 1), and a series of "higher charged" PEGylated cationic liposomes called **BC1** family formulations (Table 1). In this instance, PEGylated cationic liposome formulations were prepared using only PEG^{2000}-AAPV-Ch lipid **1**, PEG^{2000}-GPLGV-Ch lipid **2**, or the control PEG^{2000}-Ch lipid **5**. All these cationic liposome formulations were formulated by standard thin-film hydration followed by sonication to yield unilamellar vesicles. Thereafter, pDNA (specifically pEGFPLuc) was combined with selected cationic liposome formulations by direct mixing of an appropriate aliquot of nucleic acid solution with a given cationic liposome suspension followed by vigorous vortex mixing. According to our own description, the addition of pDNA to **CL1** cationic liposomes is described as resulting in the formation of **AB1** lipoplex nanoparticles. Similarly, pDNA mixing with **BC1** family PEGylated liposomes can be described as giving rise to PEGylated pDNA-nanoparticles also described as pDNA-**ABC1** nanoparticles (Scheme 3). An initial series of systematic comparative studies were then performed to review the physicochemical properties, in vitro transfection efficiencies, and cellular toxicities of these "higher charged" pDNA-nanoparticles.

Scheme 3. Schematic Diagram of a PEGylated pDNA-Nanoparticle Formulated with PEG-Peptidyl Lipids for Enzyme-Assisted Delivery of Nucleic Acids at Target Sites of Interest[a]

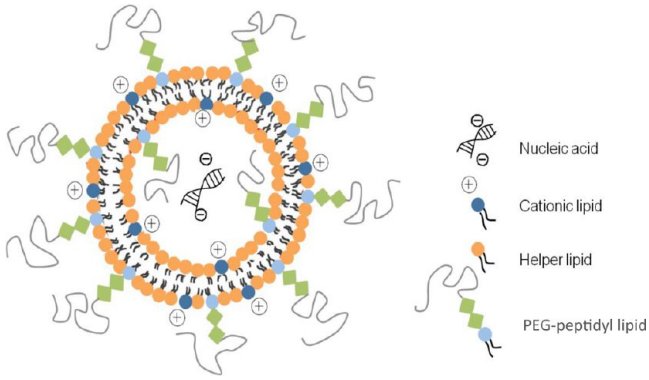

[a]The core lipoplex is illustrated as a pDNA strand located in the centre of cationic liposome. although the physical reality is of a dense multilamellar nanoparticle with pDNA entrapped between lipids in different fluid mesophase structures such as lamellar and inverse hexagonal. The same schematic diagram broadly applies for all "higher charged" pDNA-**ABCl** and "lower charged" pDNA-**ABC2** nanoparticles described in the text.

Initially, nucleic acid entrapment involving "higher charged" **CL1** cationic liposomes and a subset of **BC1** family PEGylated liposomes, prepared with PEG^{2000}-AAPV-Ch **1**, PEG^{2000}-GPLGV-Ch **2**, or the control PEG^{2000}-Ch lipid **5**, was investigated in order to determine optimal mixing ratios for maximum nucleic acid entrapment. Results of propidium iodide (PI) entrapment assays are shown for pDNA entrapment by **AB1** lipoplex nanoparticles or selected pDNA-**ABC1** nanoparticles (Figure 2a). Data show clearly that all "higher charged" cationic liposomes were able to mediate near-quantitative pDNA entrapment at a lipid/pDNA ratio of 12:1

dx.doi.org/10.1021/bc300419g | Bioconjugate Chem. 2013, 24, 343−362

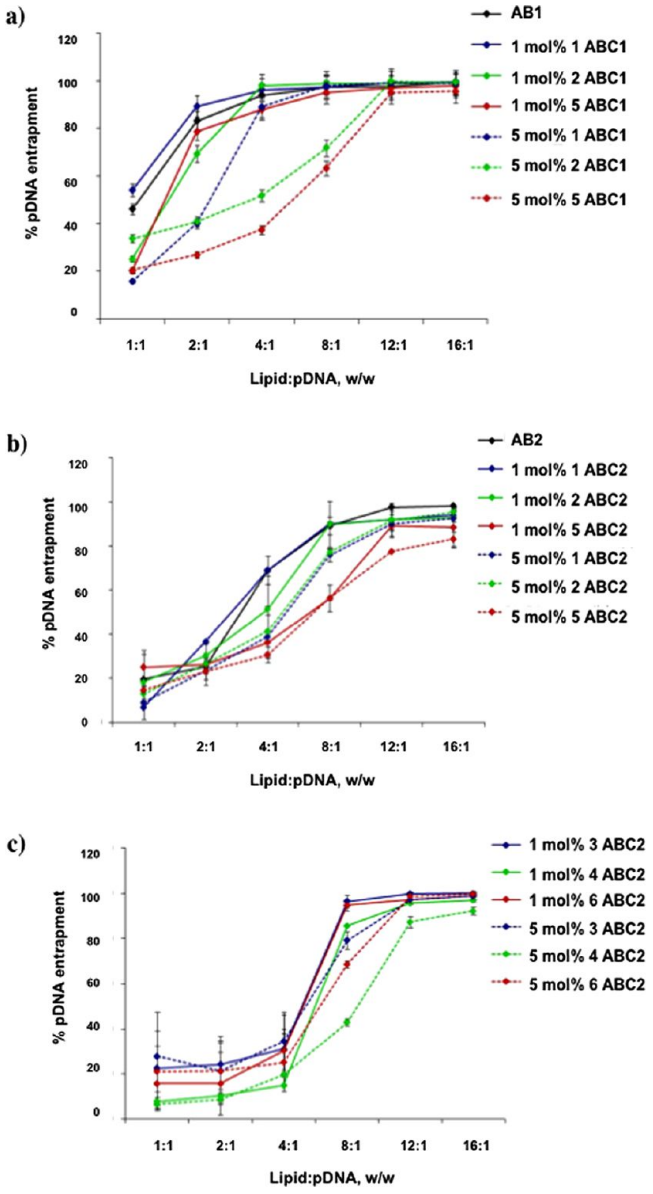

Figure 2. Entrapment of pDNA measured by propidium iodide (PI) fluorescence assay as a function of lipid/pDNA charge ratio: (a) "higher charged" pDNA-**AB1** lipoplex nanoparticle mediated entrapment of pDNA is compared with entrapments mediated by pDNA-**ABC1** nanoparticles formulated with 1 or 5 mol % PEG^{2000}-AAPV-Ch **1**, PEG^{2000}-GPLGV-Ch **2**, or PEG^{2000}-Ch **5**; (b) "lower charged" pDNA-**AB2** lipoplex nanoparticle mediated entrapment of pDNA is compared with entrapments mediated by pDNA-**ABC2** nanoparticles formulated with 1 or 5 mol % PEG^{2000}-AAPV-Ch **1**, PEG^{2000}-GPLGV-Ch **2**, or PEG^{2000}-Ch **5**; (c) comparison with entrapments mediated by pDNA-**ABC2** nanoparticles formulated with 1 or 5 mol % of lipids PEG^{2000}-AAPV-C18 **3**, PEG^{2000}-GPLGV-C18 **4**, or PEG^{2000}-C18 **6**. In all cases final [pDNA] was 1 μg/incubation.

w/w even with 5 mol % PEGylation. This result was confirmed by data obtained by gel retardation assays (Figure 3a). Accordingly, all "higher charged" pDNA-nanoparticles were prepared with a lipid/pDNA ratio of 12:1 w/w for future experiments (this corresponds with a lipid/pDNA charge ratio of approx 4). Following this, photon correlation spectroscopy (PCS) and ζ-potential measurements were made before and after the addition of pDNA (lipid/pDNA ratio of 12:1 w/w) (Figure 4a). In each case, the entrapment of pDNA resulted in a modest increase in size; by contrast, the addition of pDNA and an increase in PEGylation levels acted in concert to suppress ζ-potentials from 30 to 40 mV to 10 mV.

Transfection Properties of "Higher Charged" pDNA-Nanoparticles. Transfections mediated by **AB1** lipoplex nanoparticles or selected pDNA-**ABC1** nanoparticles were investigated. Initial studies were considered with monocytic cell lines, such as U937 and THP-1 that secrete HLE upon phorbol 12-myristate 13-acetate (PMA) stimulation. However, such suspension cell lines can be difficult to transfect due to the likelihood of reduced contact between nanoparticles and cell membranes. Accordingly, in view of the fact that elevated levels of HLE are associated with tumor progression and development in many solid cancers, we selected an adherent MCF-7 (a human breast adenocarcinoma) cell line for transfection experiments. MCF-7 transfection experiments were also conducted in the presence of added exogenous HLE, just in case endogenous production levels were too low. Otherwise, alternative transfection experiments were performed using the HT1080 (human fibrosarcoma) cell line that is known to express substantial amounts of extracellular MMP-2.[11] All transfection experiments were performed with transfection periods of up to 6 h for MCF-7 cells and of up to 24 h for HT1080 cells, followed by 24 h incubation at 37 °C, with 10% CO_2. During transfection, nanoparticles were administered to cells in media containing 10% FCS in order to provide for a more "in vivo"-like transfection environment and in order to ensure that conditions were optimal for enzyme activities. MCF-7 transfections mediated by "higher charged" **AB1** lipoplex nanoparticles were then compared with transfections mediated by "higher charged" pDNA-**ABC1** nanoparticles formulated using PEG^{2000}-AAPV-Ch **1** or the control PEG^{2000}-Ch lipid **5** (Figure 5a left). Alternatively, HT1080 transfections mediated by **AB1** lipoplex nanoparticles were compared with transfections mediated by pDNA-**ABC1** nanoparticles formulated using PEG^{2000}-GPLGV-Ch **2** or the control PEG^{2000}-Ch lipid **5** (Figure 5a right).

In MCF-7 cells, data very cleanly show that pDNA-**ABC1** nanoparticles were more effective agents of transfection than **AB1** lipoplex nanoparticles. Critically, the formulation of PEGylated pDNA-nanoparticles with PEG^{2000}-AAPV-Ch **1** led to a substantial one-log enhancement in transfection efficiency compared with **AB1** lipoplex nanoparticle-mediated transfection, and a 2−3-fold enhancement relative to transfection mediated by corresponding PEGylated pDNA-nanoparticles formulated with only PEG^{2000}-Chol **5**. In contrast, in HT1080 cells, pDNA-**ABC1** nanoparticles were more effective agents of transfection than **AB1** lipoplex nanoparticles only when the PEGylated pDNA-nanoparticles were formulated with PEG^{2000}-GPLGV-Ch **2**, and even then only by between 1.2- and 2.5-fold. Other PEGylated pDNA-nanoparticles formulated with control lipid PEG^{2000}-Ch **5** were 3−10-fold less effective than PEGylated pDNA-nanoparticles formulated with PEG^{2000}-GPLGV-Ch **2** and also significantly less transfection competent than **AB1** lipoplex nanoparticles. In spite of this generally good transfection profile, **AB1** lipoplex and pDNA-**ABC1** nanoparticles proved unstable with respect to aggregation during incubation at 37 °C, even in the presence of just 10% serum, as shown by PCS monitoring of nanoparticle size increases as a function of time (Figure 6a). Those PEGylated pDNA-nanoparticles with 5 mol % PEG were found to be the most stable at 37 °C during the 4 h period of incubation.

dx.doi.org/10.1021/bc300419g | *Bioconjugate Chem.* 2013, 24, 343−362

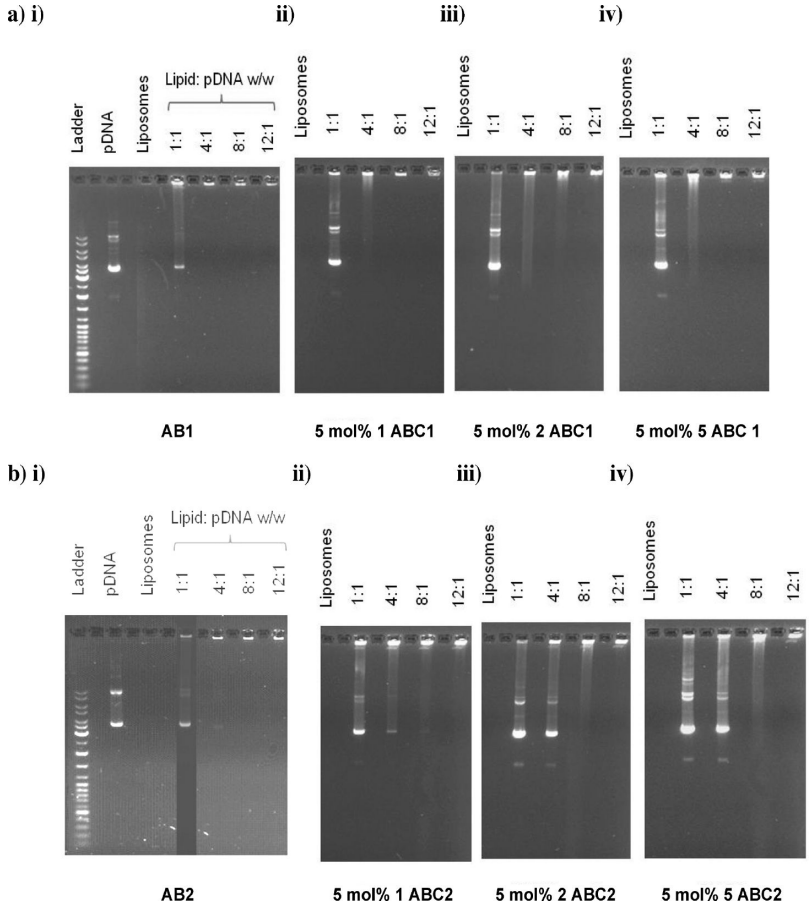

Figure 3. Agarose (0.8%) gel retardation assays to determine lipid/pDNA v/v ratios required for full pDNA retardation and therefore tight entrapment: (a) (i) retardations mediated by pDNA-**AB1** lipoplex nanoparticle formation at different w/w ratios made in comparison with naked pDNA and "higher charged" **CL1** control cationic liposomes. Remaining data show retardations mediated by pDNA-**ABCl** nanoparticles formulated at different w/w ratios from "higher charged" **BC1** PEGylated cationic liposomes prepared using 5 mol % PEG^{2000}-AAPV-Ch **1** (ii), 5 mol % PEG^{2000}-GPLGV-Ch **2** (iii), or 5 mol % PEG^{2000}-Ch **5** (iv); (b) repeat of (a) with "lower charged" **CL2** and PEGylated **BC2** cationic liposomes also formulated with **1**, **2**, or **5**: essentially identical data were obtained when retardations were observed mediated by pDNA-**ABC2** nanoparticles formulated at different w/w ratios from "lower charged" **BC2** cationic liposomes prepared using 5 mol % of PEG^{2000}-AAPV-C18 **3**, PEG^{2000}-GPLGV-C18 **4**, or PEG^{2000}-C18 **6**, respectively. Electrophoresis was performed at 65 mV for 30 min and the gels were visualized under UV light using Alliance 4.7 UVITEC Cambridge. In all cases, final [pDNA] was 0.4 μg pDNA/well.

Physical and Transfection Properties of "Lower Charged" pDNA-Nanoparticles. Nanoparticles with higher ζ-potentials are often associated with efficient transfection due to increased cell membrane association and improved intracellular trafficking. Although a decrease in effective charge may significantly diminish their transfection activity, "lower charged" nanoparticles will exhibit extended circulation half-lives.[25,36] Zelphati et al. have also shown previously that the binding of negatively charged FCS components (such as bovine serum albumin [BSA], lipoproteins, fibrinogen, and heparin) to lipoplex nanoparticles dramatically reduces transfection levels. Two possible mechanisms have been suggested: (i) destabilization of nanoparticle structures upon interaction with serum components, thus inducing dissociation of pDNA from the complexes; and (ii) charge neutralization leading to colloidal destabilization and aggregation.[37] The reduction in surface charge, as a result of the surface adsorption of serum proteins, could also weaken the electrostatic interaction required for cell association and thereby reduce pDNA delivery.[37,38] Hence, from the therapeutic point of view in vivo, an efficient nucleic delivery system should be a compromise between good stability in the blood circulation and efficient transfection. Therefore, two series of "lower charged" pDNA-nanoparticles were formulated and studied. These were formulated by the addition of pDNA to cationic liposomes **CL2**, thereby deriving **AB2** lipoplex nanoparticles, or else to **BC2** family PEGylated liposomes (Table 2), hence leading to pDNA-**ABC2** family nanoparticles formulations. **ABC2** family nanoparticles were prepared using either PEG^{2000}-AAPV-Ch **1**, PEG^{2000}-GPLGV-Ch **2**, and control PEG^{2000}-Ch **5**, or PEG^{2000}-AAPV-C18 **3**, PEG^{2000}-GPLGV-C18 **4**, and control PEG^{2000}-C18 **6**.

In order to form "lower charged" pDNA-**ABC2** family nanoparticles, minimization of the surface charge could be generally achieved by decreasing the amount of the cationic lipid incorporated in the liposome formulation, as long as there is good association with nucleic acids. Consequently, the mol % of DODAG **7** was reduced to 20 mol %, while cholesterol **9** was retained at 30 mol %, and DOPC **8** was used as the other major lipid for reasons already given. Physicochemical properties were investigated as previously including entrapment efficiency (Figure 2b,c), nanoparticle size, and ζ-potential (Figure 4b), plus in vitro transfection (Figure 5b,c). As with "higher charged" pDNA-nanoparticles, so with "lower charged" pDNA-nanoparticles. Data showed clearly that all "lower charged"

dx.doi.org/10.1021/bc300419g | *Bioconjugate Chem.* 2013, 24, 343−362

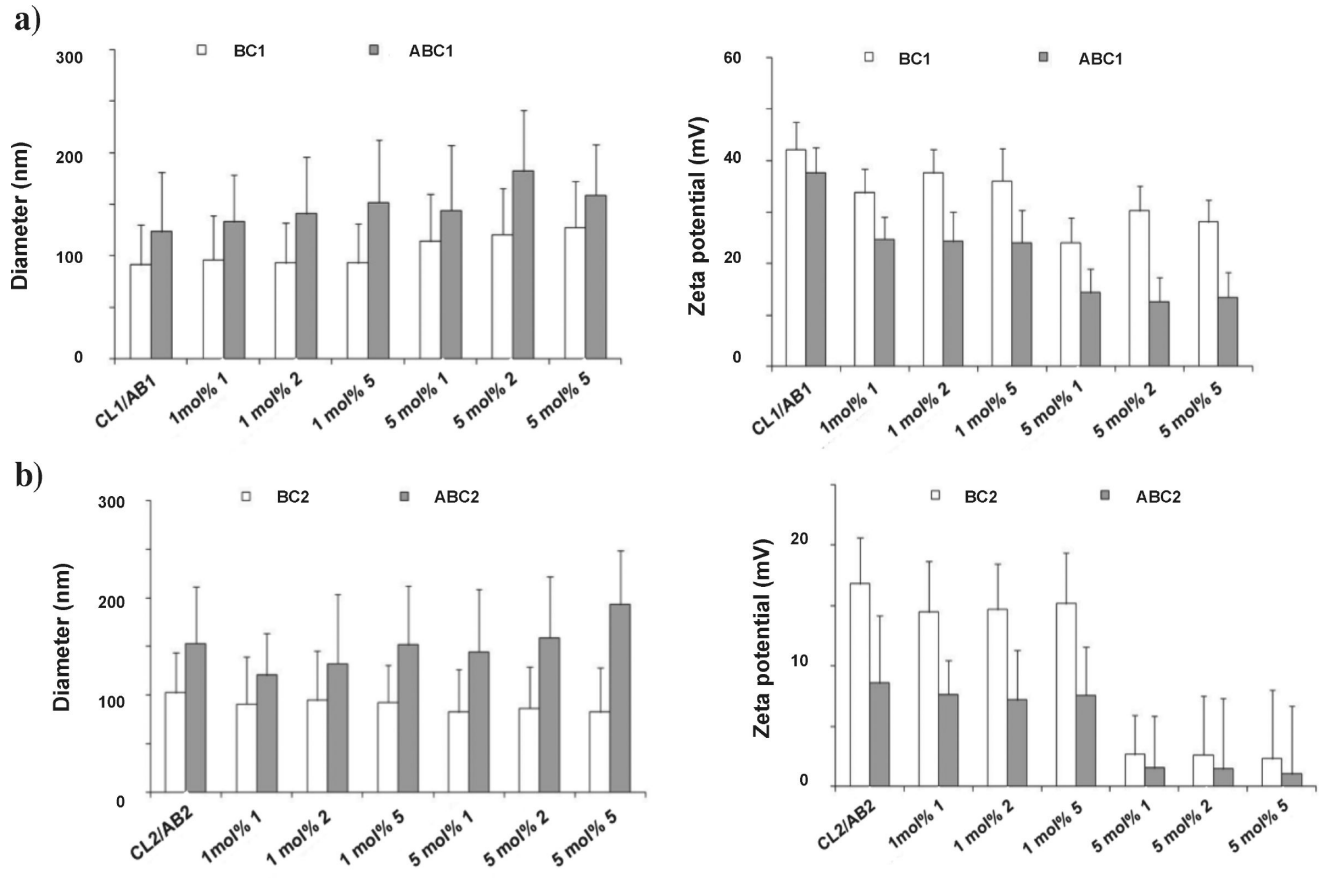

Figure 4. Average nanoparticle diameters and ζ-potentials of cationic liposomes and pDNA nanoparticles where the latter were all formulated with a lipid/pDNA w/w ratio of 12: (a) diameters (left) and ζ-potentials (right) of "higher charged" **CL1** and PEGylated **BC1** family cationic liposomes compared alongside data from corresponding pDNA-**AB1** lipoplex or pDNA-**ABC1** nanoparticles as indicated. PEGylated **BC1** family cationic liposomes and corresponding pDNA-**ABC1** nanoparticles were formulated with 1 or 5 mol % of PEG^{2000}-AAPV-Ch **1**, PEG^{2000}-GPLGV-Ch **2**, or PEG^{2000}-Ch **5** as indicated; (b) repeat of (a) showing data obtained with "lower charged" **CL2** and PEGylated **BC2** family cationic liposomes compared alongside data from corresponding pDNA-**AB2** lipoplex or pDNA-**ABC2** nanoparticles that were formulated using **1**, **2**, or **5** as indicated; essentially identical data were obtained using pDNA-**ABC2** nanoparticles formulated using PEGylated **BC2** cationic liposomes that were prepared from either PEG^{2000}-AAPV-C18 **3**, PEG^{2000}-GPLGV-C18 **4**, or PEG^{2000}-C18 **6**, respectively; total lipid concentration used was 0.5 mg/mL throughout all measurements.

cationic liposomes were able to mediate near-quantitative pDNA entrapment at a lipid/pDNA ratio of 12:1 w/w even with 5 mol % PEGylation. This result was confirmed by data obtained by gel retardation assays (Figure 3b). Accordingly, all "lower charged" pDNA-nanoparticles were prepared with a lipid/pDNA ratio of 12:1 w/w for future experiments (this corresponds with a lipid/pDNA charge ratio of approx 2).

Unsurprisingly perhaps, the entrapment of pDNA resulted in a modest increase in size (lipid/pDNA ratio of 12:1 w/w), although the ζ-potentials of 5 mol % PEGylated pDNA-nanoparticles were now reduced to as low as 1−2 mV (Figure 4b). In vitro transfection of MCF7 and HT1080 cells was then studied as before (Figure 5b,c). Those pDNA-**ABC2** nanoparticles formulated with PEG^{2000}-peptidyl-lipids **1**, **2**, **3**, or **4** mostly showed better levels of transfection than positive control lipoplex nanoparticles **AB2** even with 5 mol % levels of PEGylation. Significant transfection differentials were also observed in comparison to transfections mediated by appropriate control pDNA-**ABC2** nanoparticles formulated with control PEG^{2000}-lipids **5** or **6**. Interestingly, MMP-2 responsive "lower-charged" pDNA-**ABC2** nanoparticles prepared with PEG^{2000}-GPLGV-C18 **4** were almost 1 log order more effective at the transfection of MMP-2 expressing HT1080 cell lines than corresponding nanoparticles prepared with PEG^{2000}-GPLGV-Ch **2** (compare Figure 5b right and c right). On the other hand, HLE responsive "lower-charged" pDNA-**ABC2** nanoparticles prepared with PEG^{2000}-AAPV-Ch **1** were almost 1 log order more effective at transfection of MCF-7 cell lines (in the presence of added HLE) than corresponding nanoparticles prepared with PEG^{2000}-AAPV-C18 **3** (compare Figure 5b left and c left).

Otherwise, in nanoparticle stability studies, although **AB2** lipoplex nanoparticles were found too unstable in general and pDNA-**ABC2** nanoparticles with 1 mol % PEG lipid were only moderately unstable with respect to aggregation, "lower charged" pDNA-**ABC2** nanoparticles with 5 mol % PEG lipid were found to be completely stable with respect to aggregation during 4 h incubation at 37 °C in the presence of 10% serum (Figure 6b,c). Furthermore, "lower-charged" pDNA-**ABC2** nanoparticles formulated with 5 mol % PEG^{2000}-peptidyl-C18 lipids **3** (or **4**, data not shown) were found remarkably stable with respect to aggregation even in the presence of 80% FCS for 4 h at 37 °C (Figure 6d). Finally, LDH and MTT toxicity assays revealed that "lower-charged" pDNA-**ABC2** nanoparticles prepared with lipid/pDNA w/w ratios of 12:1 w/w were barely toxic to cells (Supporting Information Figure S1

dx.doi.org/10.1021/bc300419g | *Bioconjugate Chem.* 2013, 24, 343−362

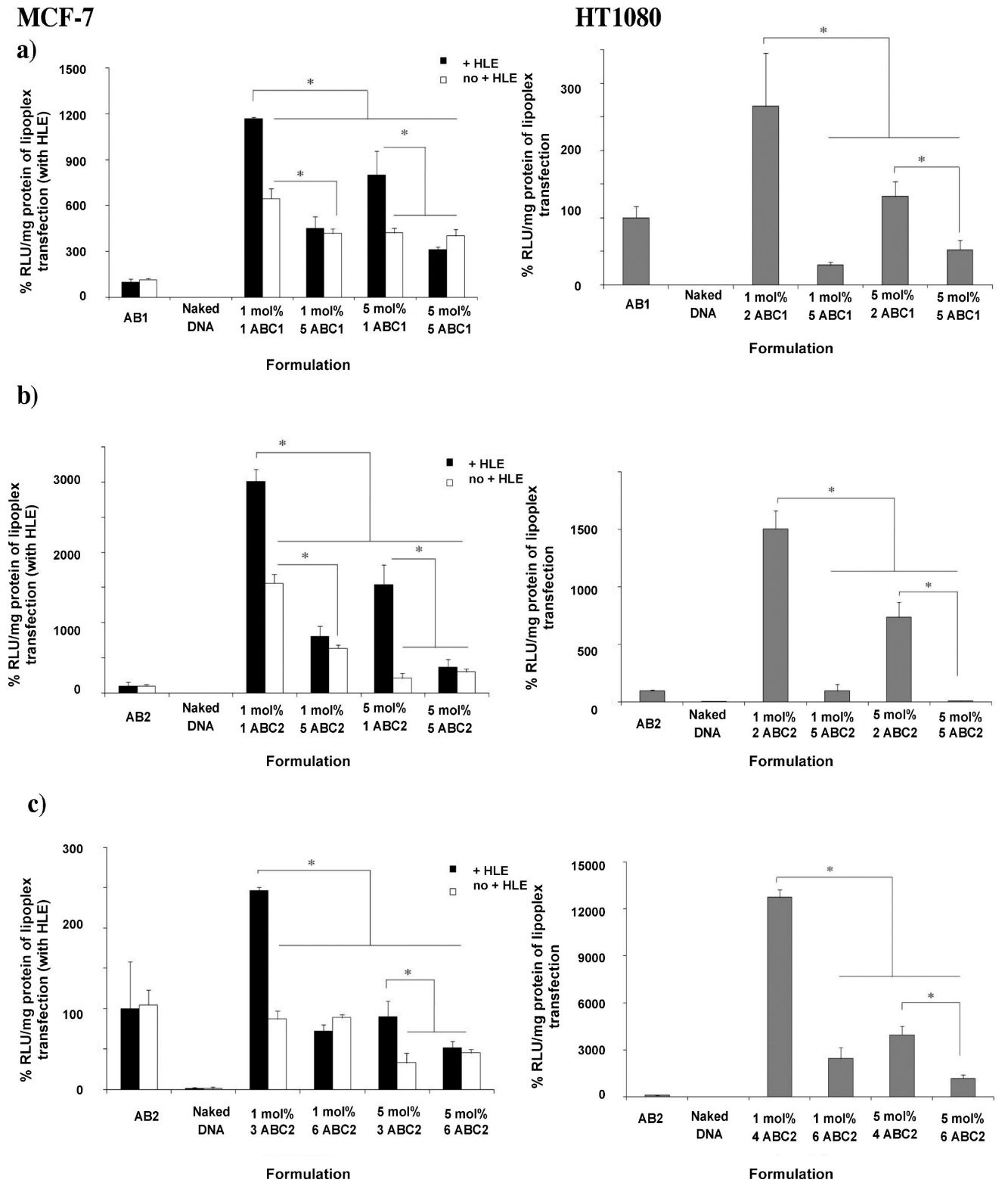

Figure 5. Differential luciferase expression levels following pDNA-nanoparticle mediated transfection of MCF-7 cells (in the presence or absence of added HLE) or of HT1080 cells: (a) differential transfection of MCF-7 cells (left) or HT1080 cells (right) post administration of "higher charged" pDNA-**AB1** lipoplex nanoparticle or naked pDNA controls, compared with data obtained post administration of pDNA-**ABC1** nanoparticles formulated either with 1 or 5 mol % of PEG^{2000}-AAPV-Ch **1**, PEG^{2000}-GPLGV-Ch **2**, or PEG^{2000}-Ch **5** as indicated; (b) same as (a) except that transfections being compared were mediated by "lower charged" pDNA-**AB2** and pDNA-**ABC2** nanoparticles formulated from the same PEG^{2000}-peptidyl-lipids as in (a); (c) same as (b) except that transfections compared were mediated by "lower charged" pDNA-**AB2** and pDNA-**ABC2** nanoparticles that were formulated with either 1 or 5 mol % of PEG^{2000}-AAPV-C18 **3**, PEG^{2000}-GPLGV−C18 **4**, or PEG^{2000}-C 18 **6** as indicated: in each case, transfection efficiency is expressed as % RLU/mg protein of lipoplex nanoparticle positive control treatment. Each result represents the mean ± SD (n = 3). * indicates $p < 0.05$: [pDNA] was 1 μg/well.

dx.doi.org/10.1021/bc300419g | *Bioconjugate Chem.* 2013, 24, 343−362

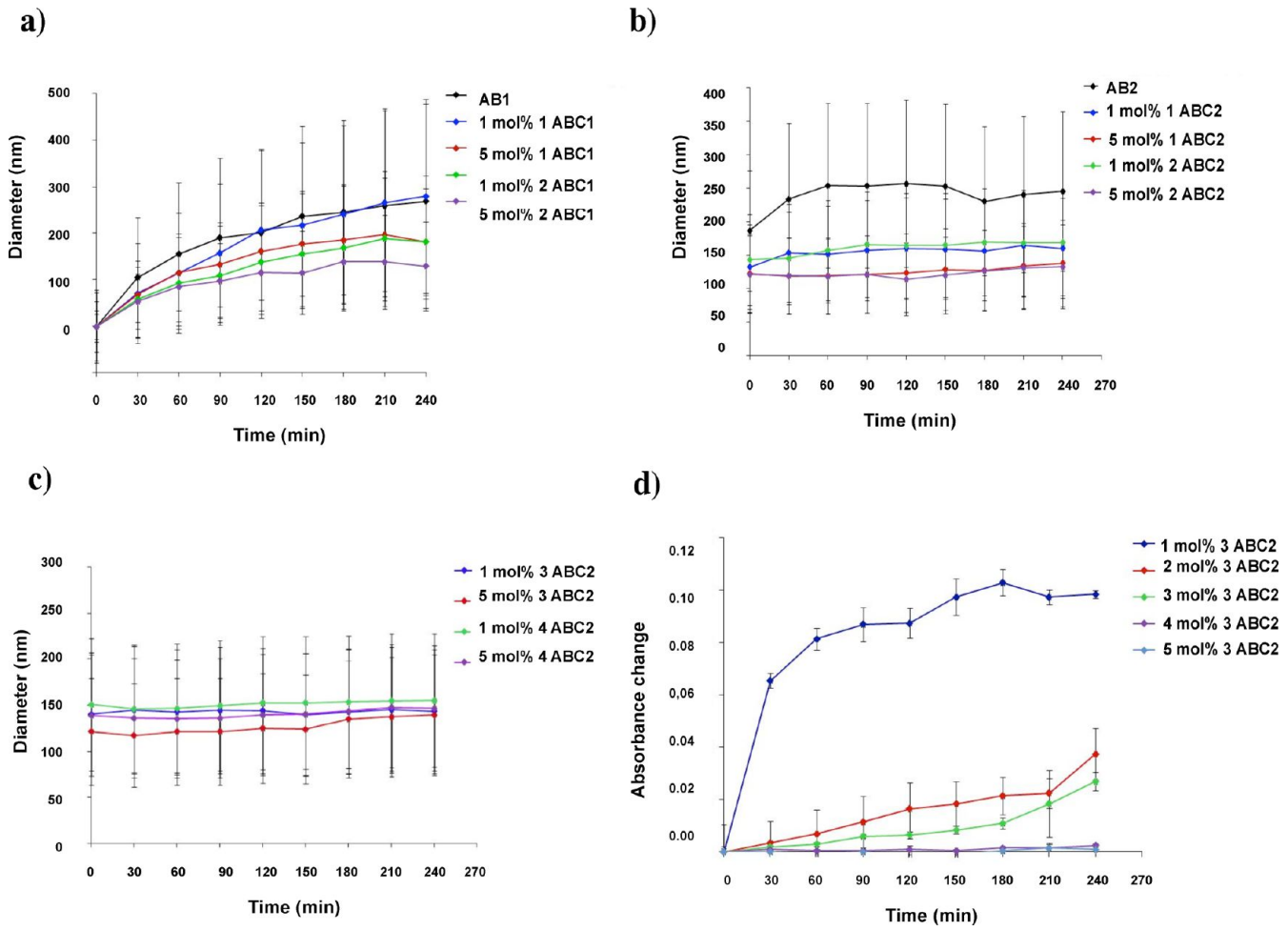

Figure 6. Nanoparticle colloidal stabilities in presence of FCS: (a) change in nanoparticle diameters with incubation time in the presence of 10% FCS w/v exhibited by "higher charged" pDNA-**AB1** lipoplex nanoparticles, and pDNA-**ABC1** nanoparticles formulated with 1 or 5 mol % of either PEG^{2000}-AAPV-Ch **1** or PEG^{2000}-GPLGV-Ch **2** as indicated. pDNA-nanoparticles were prepared at lipid to pDNA 12:1 w/w, 1 μg pDNA/incubation; (b) repeat of (a) but with "lower charged" pDNA-**AB2** lipoplex nanoparticles, and pDNA-**ABC2** nanoparticles formulated with 1 or 5 mol % of either PEG^{2000}-AAPV-Ch **1** or PEG^{2000}-GPLGV-Ch **2** as indicated; (c) repeat of (a) with alternative "lower charged" pDNA-**ABC2** nanoparticles formulated with 1 or 5 mol % of either PEG^{2000}-AAPV-C18 **3** or PEG^{2000}-GPLGV-C18 **4** as indicated; (d) change in nanoparticle diameters determined by light scattering changes with incubation time in the presence of 80% FCS w/v exhibited by "lower charged" pDNA-**ABC2** nanoparticles formulated with 1 to 5 mol % of PEG-AAPV-C18 **3**; pDNA-nanoparticles were prepared at lipid to pDNA 12:1 w/w, 1 μg pDNA/incubation.

and Figure S2), and certainly no more so than Lipofectamine2000–pDNA lipoplex nanoparticles prepared at a similar lipid/pDNA w/w ratio.[22]

Overall, these transfection data obtained with "lower charged" pDNA-**ABC2** nanoparticles in particular are completely consistent with the correct operation of an enzyme-assisted nanoparticle triggerability mechanism. Transfections mediated by pDNA-**ABC2** nanoparticles even outperformed transfections effected by positive control **AB2** lipoplex nanoparticles. Therefore, the inhibitory effects of PEGylation upon transfection are clearly alleviated by the presence of enzymatic cleavage sequences. Accordingly, our transfection and stability data (Figures 5 and 6) are entirely consistent with a mechanism of transfection that benefits from an enzyme-assisted boost when enzyme cleavage sequences are present in nanoparticle formulations. Logically, the boost could derive from one of two possibilities: (1) Enzyme-assisted cleavage of peptide linkages could be taking place thereby liberating PEG moieties from nanoparticle surfaces but leaving sufficient PEG to prevent colloidal instability. Such partial removal of PEG would then lead to the exposure of peptide moieties at nanoparticle surfaces with *N*-terminal positive charges that could promote cellular internalization. Indeed, nanoparticle surface-exposed peptides and proteins themselves are already known to promote nonspecific enhanced cell uptake for reasons that remain to be fully established.[39] (2) Alternatively, the peptide sequences themselves could act as temporary sequestration/binding sites for enzymes that over time could hydrolyze the linkage leading to PEG loss, but in the shorter term allow proteins to coat the nanoparticle surface and promote transfection efficiency in a similar way to that recounted in the description pertinent to the possibility (1) outlined above.

Furthermore, there is the possibility that FCS may be able to effect nonspecific cleavage of peptide linkages. However, this does not appear to be much of a problem given that pDNA-**ABC1** and pDNA-**ABC2** nanoparticles formulated with 5 mol % PEG^{2000}-peptidyl lipids **1**, **2**, **3**, or **4** were consistently mediating transfections more effectively than corresponding

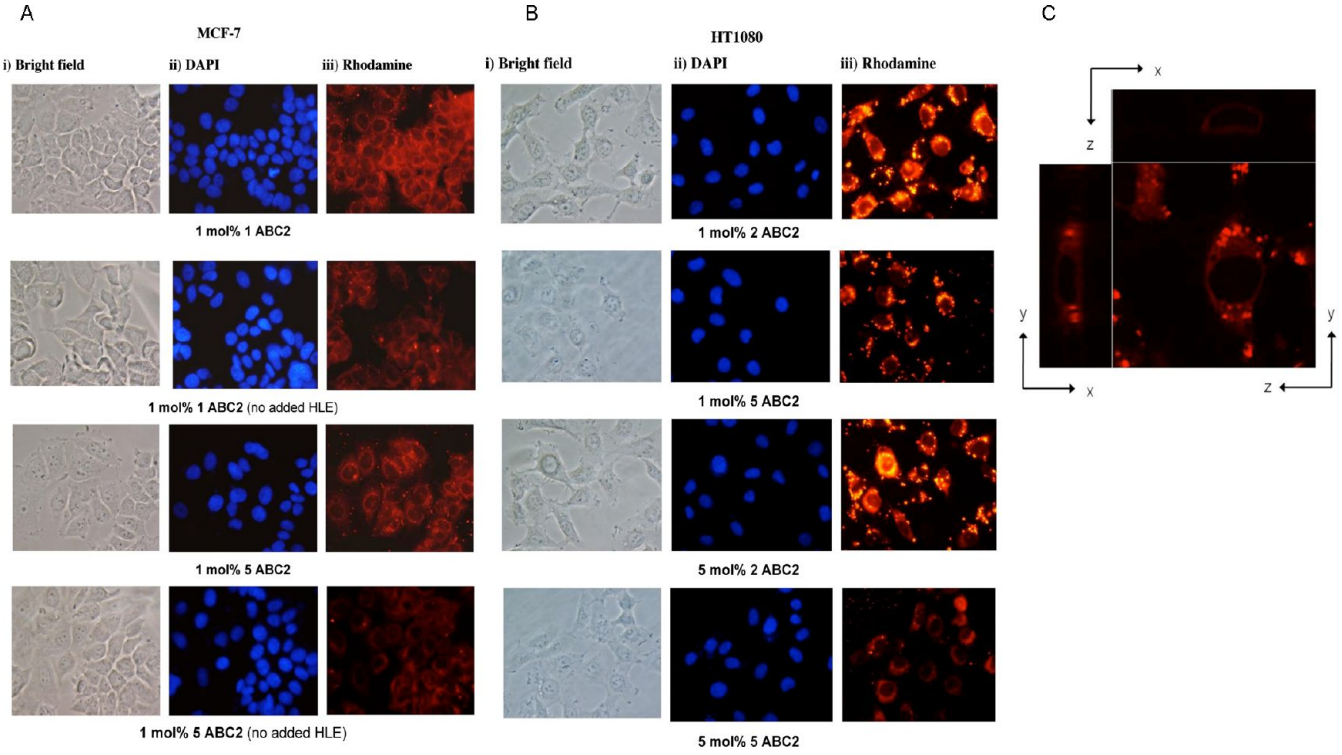

Figure 7. Fluorescence microscopy images (40× magnifications) of MCF-7 or HT1080 cells after incubation with rhodamine labeled nanoparticles: (a) results obtained with MCF-7 cells (in the presence or absence of HLE as indicated) treated with "lower charged" pDNA-**ABC2** nanoparticles formulated with 1 mol % of PEG^{2000}-AAPV-Ch **1** or control PEG^{2000}-Ch **5**. All formulations were prepared at lipid to pDNA 12:1 w/w; three views were obtained for each formulation: (i) bright field, (ii) DAPI stained nuclei, and (iii) rhodamine labeled image. Comparable data were obtained if nanoparticles were formulated with 1 mol % PEG^{2000}-AAPV-C18 **3** or control PEG^{2000}-C18 **6**; (b) repeat of (a) with results obtained with HT1080 cells treated with "lower charged" pDNA-**ABC2** nanoparticles formulated with 1 or 5 mol % of PEG^{2000}-GPLGV-Ch **2**, or control PEG^{2000}-Ch **5** as indicated. Comparable data were obtained if nanoparticles were formulated with 1 or 5 mol % of PEG^{2000}-GPLGV-C18 **4** or control PEG^{2000}-C18 **6**; (c) confocal microscopy image (40× magnification) of rhodamine labeled HT1080 cells after incubation with pDNA-**ABC2** nanoparticles formulated with 1 mol % PEG^{2000}-GPLGV-Ch **2**; a "*z*" stack illustrates a cross section through labeled HT1080 cells. In each case, total lipid was 48 μg/well.

control pDNA-**ABC1** and pDNA-**ABC2** nanoparticles formulated with 5 mol % of PEG^{2000}-lipids **5** or **6**.

Accordingly, although "higher-charged" pDNA-**ABC1** nanoparticles enhanced transfection efficiency reasonably well in the presence of the corresponding enzymes, their lack of colloidal stability in medium (containing 10% FCS) was considered to be a limiting characteristic. On the other hand, "lower charged" pDNA-**ABC2** nanoparticles with their lower surface charge (ζ-potential) (Figure 4a,b) were considered of more potential utility especially in vivo given their improved colloidal stability and their potentially lower susceptibility to opsonization and macrophage uptake consistent commensurate with increased general biological stability.[40,41] In toto, the combination of transfection and stability data further suggested to us that "lower-charged" pDNA-**ABC2** nanoparticles formulated with PEG^{2000}-peptidyl-C18 lipids **3** or **4** (most especially **4**) could be useful platforms for the development of proof of concept pDNA-based therapeutic approaches for the treatment of cancers in vivo by enzyme-assisted transfection.

Imaging of Cellular Uptake by Fluorescence Microscopy. Fluorescence microscopy was employed to visualize the cellular internalization of a selection of our PEGylated pDNA nanoparticles. Nanoparticles were prepared with 1 mol % of the fluorescent DOPE-Rhoda for this purpose, enough for visualization but not so much to perturb the nanoparticle structure. Initially, pDNA-**ABC2** nanoparticles were formulated with 1 mol % PEG^{2000}-AAPV-Ch **1** or PEG^{2000}-Ch **5**. These nanoparticles were incubated with MCF-7 for 6 h (the same uptake period as in the transfection study) and excess nanoparticles were removed at the end of the incubation period. After the cells were fixed, their nuclei were further stained using DAPI, for nuclear staining.[42] Nanoparticles were able clearly to enter cells (Figure 7a) in all cases and disperse into the cytoplasm. However, the magnitude of cellular entry (in proportion to fluorescence image intensity) and the degree of intracellular distribution varied significantly. Gratifyingly, the variations correlated closely with the outcomes of transfection experiments (Figure 5b left). In another microscopy experiment, we compared transfections mediated by pDNA-**ABC2** nanoparticles formulated with 1 and 5 mol % of PEG^{2000}-GPLGV-Ch **2** or PEG^{2000}-Ch **5**. Once again, nanoparticles were able to enter cells and disperse into the cytoplasm (Figure 7b). Once again too, imaging data correlated agreeably with the outcomes of corresponding transfection experiments (Figure 5b right).

Corresponding and equivalent microscopy data (not shown) were obtained with pDNA-**ABC2** nanoparticles formulated from 1 mol % of PEG^{2000}-AAPV-C18 **3** or PEG^{2000}-C18 **6**, or with 1 and 5 mol % of PEG^{2000}-GPLGV-C18 **4** or PEG^{2000}-C18 **6**. Once again, microscopy data was in agreement with transfection data (Figure 5c). Therefore, the level of transfection appears proportional with the intracellular concentration and distribution in accordance with the suggestion that enzyme-assisted transfection improves nanoparticle access to

dx.doi.org/10.1021/bc300419g | *Bioconjugate Chem.* 2013, 24, 343−362

cells and cell cytoplasm (see above). Finally, in order to further examine the localization of the fluorescently labeled nanoparticles inside cells, confocal microscopy was employed post transfection with pDNA-**ABC2** nanoparticles formulated with 1 mol % of PEG^{2000}-GPLGV-Ch **2** in order to derive serial imaging throughout the cells (Figure 7c). Resulting "*z*" stack images were able to confirm proper internalization of the fluorescent label. The appearance of localized hyperintense fluorescence dots may indicate the enclosure of nanoparticles in intracellular compartments such as "late endosomes".

CONCLUSION

An initial series of systematic studies are described to review the physicochemical properties, in vitro transfection efficiencies, and cellular toxicities of "higher charged" pDNA-**ABC1** and "lower charged" pDNA-**ABC2** nanoparticles (Scheme 3). In so doing, we hoped to identify PEGylated pDNA-nanoparticles that would be both stable with respect to aggregation in biological fluids and also capable of mediating transfection with clear, unambiguous enzyme assistance in vitro. This objective appears to have been achieved (at least in part). We have identified "lower charged" pDNA-**ABC2** nanoparticles formulated with either 5 mol % PEG^{2000}-peptidyl-Ch lipids **1** and **2**, or more especially, PEG^{2000}-peptidyl-C18 lipids **3** and **4**, that are stable with respect to aggregation, of apparently minimal cellular toxicity, and exhibit transfection in vitro with clear enzyme-assistance relative to pDNA-**ABC2** nanoparticles formulated with control lipids PEG^{2000}-Ch **5** or PEG^{2000}-C18 **6** (Figures 2 to 7). Our current imaging data are in clear, qualitative support of the notion that HLE or MMP-2 enzymes boost transfection by enhancing nanoparticle uptake and intracellular trafficking relative to controls (Figure 7). However, the exact mechanism of this enzyme-assisted enhancement process is yet to be established. At this stage, we have proposed two possible alternatives. The first in which enzymes perform specific hydrolyses of peptidyl moieties, releasing or shedding[43] some PEG^{2000} chains from nanoparticle surfaces, generating "naked" surface patches that can spearhead cell uptake endocytosis with endosomolysis and hence enhance transfection efficiencies. The second in which enzymes associate with nanoparticle surfaces via specific binding to peptidyl moieties and thereby boost transfection through the nonspecifc enhancing effects of surface bound proteins on the efficiency of endocytosis and downstream endosomolysis. Either proposal is consistent with a definition of nanoparticle triggerability, namely, that a nanoparticle should be stable until target site is reached, after which local release of the encapsulated therapeutic nucleic acids takes place under the influence of an endogenous or exogeneous trigger.[6,7,43]

Further development of enzyme-assisted delivery of nucleic acids could involve increasing the sensitivity of peptide linkers to create more efficient PEG release or surface binding of proteins, which would ultimately increase pDNA transfection efficiencies and even siRNA-mediated gene knockdowns. For instance, the numbers of amino acid residues involved could be increased to improve interaction with enzyme active sites. Furthermore, peptide sequences including GPLGIAGQ[44] and GPLGVRGC[45] could be employed that have been demonstrated recently to be efficient MMP-2 target sequences. The use of such octapeptides may not only allow for more efficient removal of PEG via enzymatic cleavage of the peptide linker, but also enhance intracellular trafficking by promoting internal endosomolysis, for example. Therefore, the inclusion of bona fide biological targeting ligands attached to the surfaces of PEGylated nanoparticles could provide a further boost to functional delivery at target cells of interest.[46,47] Our data also show that the lipid moiety of PEG^{2000}-peptidyl lipids can also play a potentially important role in favoring functional delivery of nucleic acids to one set of target cells over another (Figure 5). Hence, overall we appear to have obtained proof of concept in vitro for the formulation of PEGylated pDNA-nanoparticles that possess enzyme triggerability, namely, they are primed for enzyme-assisted, functional nucleic acid delivery. Moreover, the PEGylated pDNA-nanoparticles developed should be appropriate for in vivo use given their excellent transfection and FCS stability profiles (Figures 5 to 7). A range of in vivo studies will be underway shortly.

ASSOCIATED CONTENT

Supporting Information

Additional information on "lower charged" pDNA-ABC2 nanoparticle behavior. This material is available free of charge via the Internet at http://pubs.acs.org.

AUTHOR INFORMATION

Corresponding Author

*E-mail addresses: a.miller07@btinternet.com and andrew.d.miller@kcl.ac.uk.

Notes

The authors declare no competing financial interest.

ACKNOWLEDGMENTS

We thank the Mitsubishi Chemical Corporation and IC-Vec Ltd for the provision of financial support for the Imperial College Genetic Therapies Centre. P.Y. wishes to thank the Royal Thai Government for a Ph.D. studentship. S. F. wishes to thank the Swiss Government for a National Science Foundation award.

ABBREVIATIONS

pDNA, plasmid DNA; PEG, poly(ethylene glycol); HLE, human leukocyte elastase; MMP-2, matrix metalloproteinase-2; PEG^{2000}-NHS ester, α-Methoxy-PEG^{2000}-ω-*N*-hydroxysuccinide; DODAG, *N*′,*N*′-dioctadecyl-*N*-4,8-diaza-10-aminodecanoylglycylamide; DOPC, dioleoyl-L-α-phosphatidylcholine; Chol, cholesterol; Fmoc, Fluorenylmethyloxycarbonyl; HBTU, 2-(1*H*-benzotriazole-1-yl)-1,1,3,3-tetramethyluronium hexafluorophosphate; DIPEA, diisopropylethylamine; HOBt, hydroxybenzotriazole; DMAP, dimethylaminopyridine; DMF, dimethylformamide; HEPES, 2-[4-(2-hydroxyethyl)piperazin-1-yl]ethanesulfonic acid; PI, propidium iodide; FCS, fetal calf serum; DMEM, Dulbecco's Modified Eagle's Medium; MTS assay, (3-(4,5-dimethylthiazol-2-yl)-5-(3-carboxymethoxyphenyl)-2-(4-sulfophenyl)-2*H*-tetrazolium) assay; LDH assay, lactate dehydrogenase assay; PBS, phosphate-buffered saline; DOPE-Rhoda, dioleoyl-L-α-phosphatidylethanolamine-*N*-(lissamine rhodamine B sulfonyl); HPLC, high-performance liquid chromatography; DOPE, dioleoyl-L-α-phosphatidylethanolamine; PMA, phorbol 12-myristate 13-acetate; DAPI, 4′,6-diamidino-2-phenylindole

REFERENCES

(1) Miller, A. D. (2003) The problem with cationic liposome/micelle-based non-viral vector systems for gene therapy. *Curr. Med. Chem. 10*, 1195−1211.

(2) Fletcher, S., Ahmad, A., Perouzel, E., Heron, A., Miller, A. D., and Jorgensen, M. R. (2006) In vivo studies of dialkynoyl analogues of DOTAP demonstrate improved gene transfer efficiency of cationic liposomes in mouse lung. *J. Med. Chem. 49*, 349−357.
(3) Fletcher, S., Ahmad, A., Perouzel, E., Jorgensen, M. R., and Miller, A. D. (2006) A dialkanoyl analogue of DOPE improves gene transfer of lower-charged, cationic lipoplexes. *Org. Biomol. Chem. 4*, 196−199.
(4) Fletcher, S., Ahmad, A., Price, W. S., Jorgensen, M. R., and Miller, A. D. (2008) Biophysical properties of CDAN/DOPE-analogue lipoplexes account for enhanced gene delivery. *ChemBioChem 9*, 455−463.
(5) Tagawa, T., Manvell, M., Brown, N., Keller, M., Perouzel, E., Murray, K. D., Harbottle, R. P., Tecle, M., Booy, F., Brahimi-Horn, M. C., Coutelle, C., Lemoine, N. R., Alton, E. W. F. W., and Miller, A. D. (2002) Characterisation of LMD virus-like nanoparticles self-assembled from cationic liposomes, adenovirus core peptide μ (mu) and plasmid DNA. *Gene Ther. 9*, 564−576.
(6) Kostarelos, K., and Miller, A. D. (2005) Synthetic, self-assembly ABCD nanoparticles; a structural paradigm for viable synthetic non-viral vectors. *Chem. Soc. Rev. 34*, 970−994.
(7) Miller, A. D. (2008) Towards safe nanoparticle technologies for nucleic acid therapeutics. *Tumori 94*, 234−245.
(8) Miller, A. D. (2008) Synthetic nucleic acid delivery systems in gene therapy, in *Encyclopedia of Life Sciences*, J. Wiley & Sons, DOI: 10.1002/9780470015902.a0005745.pub2.
(9) Aissaoui, A., Chami, M., Hussein, M., and Miller, A. D. (2011) Efficient topical delivery of plasmid DNA to lung in vivo mediated by putative triggered, PEGylated pDNA nanoparticles. *J. Controlled Release 154*, 275−284.
(10) Drake, C. R., Aissaoui, A., Argyros, O., Serginson, J. M., Monnery, B. D., Thanou, M., Steinke, J. H. G., and Miller, A. D. (2010) Bioresponsive small molecule polyamines as non-cytotoxic alternative to polyethylenimine. *Mol. Pharmaceutics 7*, 2040−2055.
(11) Hatakeyama, H., Akita, H., Kogure, K., Oishi, M., Nagasaki, Y., Kihira, Y., Ueno, M., Kobayashi, H., Kikuchi, H., and Harashima, H. (2007) Development of a novel systemic gene delivery system for cancer therapy with a tumor-specific cleavable PEG-lipid. *Gene Ther. 14*, 68−77.
(12) Pak, C. C., Ali, S., Janoff, A. S., and Meers, P. (1998) Triggerable liposomal fusion by enzyme cleavage of a novel peptide-lipid conjugate. *Biochim. Biophys. Acta 1372*, 13−27.
(13) Pak, C. C., Erukulla, R. K., Ahl, P. L., Janoff, A. S., and Meers, P. (1999) Elastase activated liposomal delivery to nucleated cells. *Biochim. Biophys. Acta 1419*, 111−126.
(14) Han, F., and Zhu, H. G. (2010) Caveolin-1 regulating the invasion and expression of matrix metalloproteinase (MMPs) in pancreatic carcinoma cells. *J. Surg. Res. 159*, 443−450.
(15) Hyuga, S., Nishikawa, Y., Sakata, K., Tanaka, H., Yamagata, S., Sugita, K., Saga, S., Matsuyama, M., and Shimizu, S. (1994) Autocrine factor enhancing the secretion of M(r) 95,000 gelatinase (matrix metalloproteinase 9) in serum-free medium conditioned with murine metastatic colon carcinoma cells. *Cancer Res. 54*, 3611−3616.
(16) Kean, M. J., Williams, K. C., Skalski, M., Myers, D., Burtnik, A., Foster, D., and Coppolino, M. G. (2009) VAMP3, syntaxin-13 and SNAP23 are involved in secretion of matrix metalloproteinases, degradation of the extracellular matrix and cell invasion. *J. Cell. Sci. 122*, 4089−4098.
(17) Lin, S. W., Lee, M. T., Ke, F. C., Lee, P. P., Huang, C. J., Ip, M. M., Chen, L., and Hwang, J. J. (2000) TGFbeta1 stimulates the secretion of matrix metalloproteinase 2 (MMP2) and the invasive behavior in human ovarian cancer cells, which is suppressed by MMP inhibitor BB3103. *Clin. Exp. Metastasis 18*, 493−499.
(18) Lu, N., Ling, Y., Gao, Y., Chen, Y., Mu, R., Qi, Q., Liu, W., Zhang, H., Gu, H., Wang, S., Yang, Y., and Guo, Q. (2008) Endostar suppresses invasion through downregulating the expression of matrix metalloproteinase-2/9 in MDA-MB-435 human breast cancer cells. *Exp. Biol. Med. 233*, 1013−1020.
(19) Morgunova, E., Tuuttila, A., Bergmann, U., and Tryggvason, K. (2002) Structural insight into the complex formation of latent matrix metalloproteinase 2 with tissue inhibitor of metalloproteinase 2. *Proc. Natl. Acad. Sci. U.S.A. 99*, 7414−7419.
(20) Stellas, D., El Hamidieh, A., and Patsavoudi, E. (2010) Monoclonal antibody 4C5 prevents activation of MMP2 and MMP9 by disrupting their interaction with extracellular HSP90 and inhibits formation of metastatic breast cancer cell deposits. *BMC Cell Biol. 11*, 51.
(21) Wang, F. Q., So, J., Reierstad, S., and Fishman, D. A. (2005) Matrilysin (MMP-7) promotes invasion of ovarian cancer cells by activation of progelatinase. *Int. J. Cancer 114*, 19−31.
(22) Mével, M., Kamaly, N., Carmona, S., Oliver, M. H., Jorgensen, M. R., Crowther, C., Salazar, F. H., Marion, P. L., Fujino, M., Natori, Y., Thanou, M., Arbuthnot, P., Yaouanc, J.-J., Jaffres, P. A., and Miller, A. D. (2010) DODAG; a versatile new cationic lipid that mediates efficient delivery of pDNA and siRNA. *J. Controlled Release 143*, 222−232.
(23) Lee, G. Y., Park, K., Kim, S. Y., and Byun, Y. (2007) MMPs-specific PEGylated peptide-DOX conjugate micelles that can contain free doxorubicin. *Eur. J. Pharm. Biopharm. 67*, 646−654.
(24) Lv, H., Zhang, S., Wang, B., Cui, S., and Yan, J. (2006) Toxicity of cationic lipids and cationic polymers in gene delivery. *J. Controlled Release 114*, 100−109.
(25) Miller, C. R., Bondurant, B., McLean, S. D., McGovern, K. A., and O'Brien, D. F. (1998) Liposome-cell interactions in vitro: effect of liposome surface charge on the binding and endocytosis of conventional and sterically stabilized liposomes. *Biochemistry 37*, 12875−12883.
(26) Koltover, I., Salditt, T., Radler, J. O., and Safinya, C. R. (1998) An inverted hexagonal phase of cationic liposome-DNA complexes related to DNA release and delivery. *Science 281*, 78−81.
(27) Wasungu, L., and Hoekstra, D. (2006) Cationic lipids, lipoplexes and intracellular delivery of genes. *J. Controlled Release 116*, 255−264.
(28) Hong, K., Zheng, W., Baker, A., and Papahadjopoulos, D. (1997) Stabilization of cationic liposome-plasmid DNA complexes by polyamines and poly(ethylene glycol)-phospholipid conjugates for efficient in vivo gene delivery. *FEBS Lett. 400*, 233−237.
(29) Li, S., Rizzo, M. A., Bhattacharya, S., and Huang, L. (1998) Characterization of cationic lipid-protamine-DNA (LPD) complexes for intravenous gene delivery. *Gene Ther. 5*, 930−937.
(30) Stewart, L., Manvell, M., Hillery, E., Etheridge, C. J., Cooper, R. G., Stark, H., van-Heel, M., Preuss, M., Alton, E. W. F. W., and D., M. A. (2001) Physico-chemical analysis of cationic liposome-DNA complexes (lipoplexes) with respect to in vitro and in vivo gene delivery efficiency. *J. Chem. Soc., Perkin Trans. 2*, 624−632.
(31) Strijkers, G. J., Mulder, W. J., van Heeswijk, R. B., Frederik, P. M., Bomans, P., Magusin, P. C., and Nicolay, K. (2005) Relaxivity of liposomal paramagnetic MRI contrast agents. *MAGMA 18*, 186−192.
(32) Kirby, C., Clarke, J., and Gregoriadis, G. (1980) Effect of the cholesterol content of small unilamellar liposomes on their stability in vivo and in vitro. *Biochem. J. 186*, 591−598.
(33) Semple, S. C., Chonn, A., and Cullis, P. R. (1996) Influence of cholesterol on the association of plasma proteins with liposomes. *Biochemistry 35*, 2521−2525.
(34) Cooper, R. G., Etheridge, C. J., Stewart, L., Marshall, J., Rudginsky, S., Cheng, S. H., and Miller, A. D. (1998) Polyamine analogues of 3β-[N-(N′,N′-dimethylaminoethane)carbamoyl] cholesterol (DC-Chol) as agents for gene delivery. *Chem. Eur. J. 4*, 137−152.
(35) Templeton, N. S., Lasic, D. D., Frederik, P. M., Strey, H. H., Roberts, D. D., and Pavlakis, G. N. (1997) Improved DNA: liposome complexes for increased systemic delivery and gene expression. *Nat. Biotechnol. 15*, 647−652.
(36) Kamaly, N., Kalber, T., Ahmad, A., Oliver, M. H., So, P. W., Herlihy, A. H., Bell, J. D., Jorgensen, M. R., and Miller, A. D. (2008) Bimodal paramagnetic and fluorescent liposomes for cellular and tumor magnetic resonance imaging. *Bioconjugate Chem. 19*, 118−129.
(37) Zelphati, O., Uyechi, L. S., Barron, L. G., and Szoka, F. C., Jr. (1998) Effect of serum components on the physico-chemical properties of cationic lipid/oligonucleotide complexes and on their interactions with cells. *Biochim. Biophys. Acta 1390*, 119−133.

(38) Crook, K., Stevenson, B. J., Dubouchet, M., and Porteous, D. J. (1998) Inclusion of cholesterol in DOTAP transfection complexes increases the delivery of DNA to cells in vitro in the presence of serum. *Gene Ther. 5*, 137−143.
(39) Waterhouse, J. E., Harbottle, R. P., Keller, M., Kostarelos, K., Coutelle, C., Jorgensen, M. R., and Miller, A. D. (2005) Synthesis and Application of Integrin Targeting Lipopeptides in Targeted Gene Delivery. *ChemBioChem 6*, 1212−1223.
(40) Farokhzad, O. C., Jon, S., Khademhosseini, A., Tran, T. N., Lavan, D. A., and Langer, R. (2004) Nanoparticle-aptamer bioconjugates: a new approach for targeting prostate cancer cells. *Cancer Res. 64*, 7668−7672.
(41) Zeisig, R., Arndt, D., Stahn, R., and Fichtner, I. (1998) Physical properties and pharmacological activity in vitro and in vivo of optimized liposomes prepared from a new cancerostatic alkylphospholipid. *Biochim. Biophys. Acta 1414*, 238−248.
(42) Kubista, M., Akerman, B., and Norden, B. (1987) Characterization of interaction between DNA and 4′,6-diamidino-2-phenylindole by optical spectroscopy. *Biochemistry 26*, 4545−4553.
(43) Huang, L., and Liu, Y. (2011) In Vivo Delivery of RNAi with Lipid-Based Nanoparticles. *Annu. Rev. Biomed. Eng. 13*, 507−530.
(44) Terada, T., Iwai, M., Kawakami, S., Yamashita, F., and Hashida, M. (2006) Novel PEG-matrix metalloproteinase-2 cleavable peptide-lipid containing galactosylated liposomes for hepatocellular carcinoma-selective targeting. *J. Controlled Release 111*, 333−342.
(45) Harris, T. J., von Maltzahn, G., Derfus, A. M., Ruoslahti, E., and Bhatia, S. N. (2006) Proteolytic actuation of nanoparticle self-assembly. *Angew. Chem., Int. Ed. Engl. 45*, 3161−3165.
(46) Kamaly, N., Kalber, T., Thanou, M., Bell, J. D., and Miller, A. D. (2009) Folate receptor targeted bimodal liposomes for tumor magnetic resonance imaging. *Bioconjugate Chem. 20*, 648−655.
(47) Song, S., Liu, D., Peng, J., Deng, H., Guo, Y., Xu, L. X., Miller, A. D., and Xu, Y. (2009) Novel peptide ligand directs liposomes toward EGF-R high-expressing cancer cells in vitro and in vivo. *FASEB J. 23*, 1396−1404.